European Master in Biological and Chemical Engineering for a Sustainable Bioeconomy

Master thesis report

submitted to obtain the degrees of:

Master in Biology AgroSciences (BAS) of the University of Reims Champagne-Ardenne

Master of Science in Engineering of Tallinn University of Technology

Master in Integrative Biology and Physiology (BIP) of the University Paris-Saclay, operated by AgroParisTech

Implementation of Permittivity Probes to Estimate the Viable Cell Density in Bacterial Batch Culture.

Presented by: VARONA GARCÍA José Gustavo

Defended the: 06/07/2023

Supervised by: BENCHEIKH Julien

At : Procelys by Lesaffre
103 Rue Jean Jaurès, 94700 Maisons-Alfort, France.

from: 09/02/2023 to 09/08/2023

Bioceb supervisors:

BONTURI Nemailla – Tallinn University of Technology (TalTech)

SAULOU-BÉRION Claire – AgroParisTech (Université Paris-Saclay)

Confidentiality: No Privacy expiration date: N/A

Non-exclusive licence for reproduction and publication of a graduation thesis[1]

I José Gustavo Varona García

1. grant Tallinn University of Technology free licence (non-exclusive licence) for my thesis "Implementation of Permittivity Probes to Estimate the Viable Cell Density in Bacterial Batch Culture.",
(*title of the graduation thesis*)

supervised by Julien Bencheikh_____,
(*supervisor's name*)

1.1 to be reproduced for the purposes of preservation and electronic publication of the graduation thesis, incl. to be entered in the digital collection of the library of Tallinn University of Technology until expiry of the term of copyright;

1.2 to be published via the web of Tallinn University of Technology, incl. to be entered in the digital collection of the library of Tallinn University of Technology until expiry of the term of copyright.

2. I am aware that the author also retains the rights specified in clause 1 of the non-exclusive licence.

3. I confirm that granting the non-exclusive licence does not infringe other persons' intellectual property rights, the rights arising from the Personal Data Protection Act or rights arising from other legislation.

06/07/2023 (date)

[1] *The non-exclusive licence is not valid during the validity of access restriction indicated in the student's application for restriction on access to the graduation thesis that has been signed by the school's dean, except in case of the university's right to reproduce the thesis for preservation purposes only. If a graduation thesis is based on the joint creative activity of two or more persons and the co-author(s) has/have not granted, by the set deadline, the student defending his/her graduation thesis consent to reproduce and publish the graduation thesis in compliance with clauses 1.1 and 1.2 of the non-exclusive licence, the non-exclusive license shall not be valid for the period.*

Last name: Varona Garcia ……

First name: José Gustavo …….

a master's student,

declare being fully aware that copying all or part of a document, whatever it may be, published on any kind of existing medium, including the internet, constitutes a violation of copyright and outright fraud.

As a consequence, I hereby declare that my master's thesis does not contain any form of plagiarism, and I hereby certify that I have explicitly quoted, every time that I have used them, all the sources used to write my master's thesis.

Done at (city) Maisons-Alfort……, this (date) 12 June 2023……

AgroParisTech-Campus de Saclay
Direction de la formation
22 place de l'agronomie
91120 Palaiseau

Acknowledgments

This project was developed from February 9th to July 5th, 2023, in the Biotechnological Applications Laboratory of Procelys, a business unit of Lesaffre, part of the industrial site Biospringer in Maisons-Alfort, France.

Firstly, I would like to thank my supervisor at Procelys Julien Bencheikh, Application Lab Scientist, whose guidance and support have been instrumental in shaping my work. I am grateful for the insightful feedback and the throughout the course of this project. I would like to also thank Magali Cros, Biotechnological Applications Laboratory Manager, whose expertise, and knowledge broadened my perspective on the subject matter.

I would also like to extend my appreciation to my supervisors at Claire Saulou-Bérion from AgroParisTech, for her support during this period. I would like to extend my sincere gratitude to Nemailla Bonturi, supervisor at TalTech for her invaluable teaching and guidance during my studies in Tallinn.

I am deeply grateful to the European Commission and the Bioceb consortium for providing me with the scholarship that enabled me to pursue my master studies. Their support has been critical in helping me achieve my academic goals.

Finally, I would like to express my appreciation to all the individuals who have contributed in any way towards the completion of my studies. I am grateful for their support, encouragement, and assistance throughout my academic journey.

Table of Contents

Acknowledgments ..... *IV*
Table of Contents ..... *V*
Index of Tables and Figures ..... *VI*
Abstract *1*
1. Introduction *3*
1.1. Procelys 3
1.2. Probiotics 4
1.3. Cell viability and functionality 6
2. State of the art *14*
2.1. Permittivity probes use in cell culture 14
2.2. Application of permittivity probes for bacterial and yeast fermentations. 15
2.3. Bifidobacterium animalis subsp. lactis 16
2.4. Lactobacillus acidophilus 16
3. Objectives *18*
3.1. General 18
3.2. Particular 18
4. Materials and methods *19*
4.1. Strains and culture media 19
4.2. Online capacitance measurements 21
4.3. Offline viable cell density measurements 21
4.4. Other measurements 23
4.5. Correlation between viable cell density and permittivity 24
5. Results *25*
5.1. Bifidobacterium animalis subsp. lactis 25
5.2. Lactobacillus acidophilus 35
6. Discussion *43*
7. Conclusions and perspectives *45*
8. Annex ..... *IV*
8.1. Files containing the models and the coefficients IV
9. References ..... *IX*

Index of Tables and Figures

Tables

Table 1.1 Some dyes used in fluorometric flow cytometry (Adapted from Díaz et al., 2010). 9
Table 4.1 Culture media composition for the main culture of *B. lactis* and *L. acidophilus*. 20
Table 4.2 Samples for the flow cytometry calibration with the method Syto24/PI 22
Table 4.3 Samples for the flow cytometry calibration with the method cFDA/PI 23

Figures

Figure 1.1 Biotechnological applications of Procelys products (Procelys, 2023). 4
Figure 1.2. Possible distribution of mechanisms among probiotics (Hill et al., 2014). 5
Figure 1.3. Functional criteria to determine different levels of cell viability and the different states between cell viability and cell death (Díaz et al., 2010). 7
Figure 1.4 Idealized spectrum of the dielectric properties of cell suspensions and tissues (Markx & Davey, 1999). 11
Figure 1.5 Schematic representation of the β-dispersion with the key parameters of the curve (Flores-Cosío et al., 2020). 12
Figure 5.1 Offline measurements for Viable Cell Density of a 1-Liter batch culture of *B. lactis*. Viable cell density measured in the logarithm Colony Forming Units (CFU/mL) and Active Fluorescent Units (AFU/mL) with the methodology of double stain using Syto 24/PI and cFDA/PI. 25
Figure 5.2 Optical density at 600 nm of *B. lactis* growth in 1-liter batch culture. 26
Figure 5.3 Kinetics of glucose consumption (left), and acetate and lactate production (right) of a 1-Liter batch culture of *B. lactis*. 27
Figure 5.4 Microscopic observations of samples taken from a culture of *B. lactis* growing in mineral media with glucose as carbon source and yeast extract as a nitrogen source. 28
Figure 5.5 Curves of pH, injected base, and conductivity of a 1-liter batch fermentation of *B. lactis*. 29
Figure 5.6 Permittivity curves measured at 580 kHz of 4 replicates of 1-liter batch fermentation of *B. lactis*. 30
Figure 5.7 Culture media capacitance curves measured at 300 kHz of 4 replicates of 1-liter batch fermentation of *B. lactis*. 30
Figure 5.8 Linear correlation during the exponential phase of capacitance measurements at 300 kHz and offline measurements of viable cell density in Colony Forming Units (CFU/mL), and Active Fluorescent Units (AFU/mL) with the methodology of double stain using Syto 24/PI and cFDA/PI. Applied to 4 biological replicates of 1-liter batch fermentation of *B. lactis*. 31
Figure 5.9 Linear correlation during the exponential phase of capacitance measurements at 300 kHz and offline measurements of viable cell density in Colony Forming Units (CFU/mL), and Active Fluorescent Units (AFU/mL) with the methodology of double stain using Syto 24/PI and cFDA/PI. Applied to 1-liter batch fermentations of *B. lactis*. 32

Figure 5.10 Statistical performance of the non-linear models correlating the viable cell density, in CFU/mL (top), in AFU/mL using the Syto24/PI (middle) and cFDA/PI (bottom) methodologies, and the capacitance measurements in 1-liter batch fermentations of *B. lactis*. 34

Figure 5.11 Offline measurements for Viable Cell Density of a 1-Liter batch culture of *L. acidophilus*. Viable cell density measured in the logarithm Colony Forming Units (CFU/mL) and Active Fluorescent Units (AFU/mL) with the methodology of double stain using Syto 24/PI and cFDA/PI. 35

Figure 5.12 Optical density at 600 nm of *L. acidophilus* growth in 1-liter batch culture..... 36

Figure 5.13 Kinetics of glucose consumption (left), acetate and lactate production (right) of a 1-Liter batch culture of *L. acidophilus*. 37

Figure 5.14 Curves of pH, injected base, and conductivity of a 1-liter batch fermentation of *L. acidophilus*.37

Figure 5.15 Permittivity curves measured at 580 kHz of 4 replicates of 1-liter batch fermentation of *L. acidophilus*. 38

Figure 5.16 Culture media capacitance curves measured at 300 kHz of 4 replicates of 1-liter batch fermentation of *L acidophilus*..... 39

Figure 5.17 Linear correlation of capacitance measurements at 300 kHz and offline measurements of viable cell density in Colony Forming Units (CFU/mL), and Active Fluorescent Units (AFU/mL) with the methodology of double stain using Syto 24/PI and cFDA/PI. Applied to 4 biological replicates of 1-liter batch fermentation of *L. acidophilus*. 40

Figure 5.18 Linear correlation of capacitance measurements at 300 kHz and offline measurements of viable cell density in Colony Forming Units (CFU/mL), and Active Fluorescent Units (AFU/mL) with the methodology of double stain using Syto 24/PI and cFDA/PI. Applied to 1-liter batch fermentations of *L. acidophilus*. 41

Figure 5.19 Statistical performance of the non-linear models correlating the viable cell density, in CFU/mL (top), in AFU/mL using the Syto24/PI (middle) and cFDA/PI (bottom) methodologies, and the capacitance measurements in 1-liter batch fermentations of *L. acidophilus*. 42

European Master in Biological and Chemical Engineering for a Sustainable Bioeconomy

Abstract

Permittivity measures the degree of polarization of a material when an electric field is applied. The permittivity of a culture media is equivalent to the total life biomass concentration when measured with an electrical field at a frequency between 100 kHz and 3 MHZ since it will polarize the cell membranes. However, the equivalence is affected by the microbial strain and its morphology, then there is a linear correlation between the permittivity measurements and the viable cell density only during the exponential growth phase. To estimate the viable cell density outside the exponential growth phase it is necessary to build a non-linear model that considers the culture media capacitance measurements at different frequencies. This project had the objective of applying the measurement of capacitance and permittivity to estimate the viable cell density in 1-liter 24-hours batch cultures of bacterial models of industrial interest: *Bifidobacterium animalis* subsp. *lactis*, *Lactobacillus acidophilus* and *Bacillus subtilis*. The viable cell density was measured by viable cell count and flow cytometry using two methodologies of double staining, one with Syto 24 and PI, and another with cFDA and PI. For *B. lactis*, the exponential phase lasted from 4 hours to 12 hours of culture and there was a good linear correlation (R^2>0.9) of the viable cell density and the permittivity when the biological replicates were evaluated separately, but not at the same time. For *L. acidophilus* the exponential phase prolongated from 2 to 9 hours of culture and it had a good linear correlation even when the data of the biological replicates was evaluated at the same time. The non-linear models were not able to give good correlations and the relative error of each estimation reached up to 50%. This could be due to the lack of repeatability of the data obtained by the permittivity probes, possibly because they are optimized for its application in mammalian cell culture.

Abstraktne

Läbilaskvus mõõdab materjali polarisatsiooniastet elektrivälja rakendamisel. Kultuurisöötme läbilaskvus on samaväärne kogu elulise biomassi kontsentratsiooniga, kui seda mõõdetakse elektriväljaga sagedusel 100 kHz kuni 3 MHz, kuna see polariseerib rakumembraane. Samas mõjutab samaväärsust mikroobitüvi ja selle morfoloogia, siis on lineaarne korrelatsioon läbilaskvuse mõõtmiste ja elujõuliste rakkude tiheduse vahel ainult eksponentsiaalse kasvufaasi ajal. Elujõuliste rakkude tiheduse hindamiseks väljaspool eksponentsiaalset kasvufaasi on vaja luua mittelineaarne mudel, mis arvestab söötme mahtuvuse mõõtmist erinevatel sagedustel. Selle projekti eesmärk oli rakendada mahtuvuse ja läbilaskvuse mõõtmist, et hinnata elujõuliste rakkude tihedust tööstuslikku huvi pakkuvate bakterimudelite 1-liitristes 24-tunnistes partiikultuurides: *Bifidobacterium animalis subsp. lactis*, *Lactobacillus acidophilus* ja *Bacillus subtilis*. Elujõuliste rakkude tihedust mõõdeti elujõuliste rakkude arvu ja voolutsütomeetria abil, kasutades kahte topeltvärvimise metoodikat, millest üks oli Syto 24 ja PI ning teine cFDA ja PI abil. *B. lactis*'e puhul kestis eksponentsiaalne faas 4 tunnist 12 tunnini

kultiveerimiseni ning elujõuliste rakkude tiheduse ja läbilaskvuse vahel oli hea lineaarne korrelatsioon (R^2>0,9), kui replikaate hinnati eraldi, kuid mitte samal ajal. *L. acidophilus*'e puhul pikenes eksponentsiaalne faas 2-lt 9-le tunnile ja sellel oli hea lineaarne korrelatsioon isegi siis, kui samaaegselt hinnati replikaatide andmeid. Mittelineaarsed mudelid ei suutnud anda häid korrelatsioone ja iga hinnangu suhteline viga ulatus kuni 50%. See võib olla tingitud läbilaskvussondidega saadud andmete korratavuse puudumisest, võib-olla seetõttu, et need on optimeeritud selle kasutamiseks imetajate rakukultuuris.

1. Introduction

One of human's biggest challenge for the years to come is responding to the increasing demand of energy, food, and pharmaceuticals. World population reached 8 billion people recently; and it is projected to continue growing to 9.7 billion people by 2050 driven mainly by an increase in the population of developing countries mainly from sub-Saharan Africa and Central-Southern Asia (United Nations, 2022). Besides, this increased population is followed by an increase in life quality standards of the population of developing countries which will indeed increase the human need on energy and food. Unfortunately, these needs are currently addressed using fossil fuels which are quickly diminishing and causing environmental threats including ecosystem degradation and climate change (Wagemann & Tippkötter, 2019). In this context, a transition towards bioeconomy, the replacement of fossil-based products, and the development of novel solutions is necessary to address the needs of the population, to avoid further environmental degradation, to achieve the Sustainable Development Goals of the United Nations in the horizon 2030 (Papadopoulou et al., 2022).

Biotechnology can provide us with several tools that could allow us to reach those objectives. Industrial biotechnology is often regarded as a field for industrial production with reduced energy consumption, greenhouse gases emissions, and low waste generation (Yu et al., 2019). Besides, the latest developments in biotechnology and synthetic biology bring us promises of development that could positively impact the pharmaceutical industry, food and feed industries, chemical industry, and even the fuel and energy sectors in the years to come. They could bring more sustainable processes that could better follow the 12 green chemistry principles compared to the current chemical industry (Tang & Zhao, 2009). These are the reasons why it is necessary to develop the industrial biotechnology, so those promises can be materialized in the real world and help us solving the environmental and social challenges of this century.

1.1. Procelys

Lesaffre is a major player in the fermentation of microorganisms (yeasts, bacteria), with a turnover of 2.2 billion euros and product distribution in 185 countries. Established in 1853, this French family-owned company has evolved into a group with over 11,000 employees, 76 production sites, and subsidiaries across all continents. The company's mission is to feed, protect the health and well-being of as many people as possible, while preserving the planet's natural resources. Leveraging its experience and diversity, Lesaffre provides innovative solutions in the fields of baking, taste and culinary pleasure, health nutrition, and industrial biotechnology (Lesaffre, 2023).

Procelys is a Lesaffre Business Unit dedicated to biotechnology industries. It offers a range of fermentation nutrients developed to improve bacterial growth and the productivity of microorganisms

and animal cells. These nutrients, including yeast extracts, dried yeast, and yeast peptones, are designed for specific applications. Procelys has commercial offices in France, the United States, China, India, Brazil, and Singapore. It also operates biotechnological applications laboratories in France, the United States, and China (Procelys, 2023).

Figure 1.1 Biotechnological applications of Procelys products (Procelys, 2023).

1.2. Probiotics

The antibiotics resistance is one of the biggest threats to global public health and food safety. In 2014 it was estimated that that antibiotic resistance caused 700 thousand deaths every year minimum and that by 2050 it will cause 10 million deaths per year worldwide, becoming the first cause of death, and affecting mainly African and Asian countries in development (O'Neill, 2014). Furthermore, it is estimated a loss between 2% and 3% of the global GDP, between 60 and 100 trillion USD for 2050 (O'Neill, 2014).

To tackle the antibiotic resistance several alternatives have been proposed including vaccines, antibodies, bacteriophages treatment, immune stimulation, and probiotics. These last have been proposed for prevention as well as for treatment (Czaplewski et al., 2016),

Probiotics are defined as living organisms that, when administered in adequate amounts, confer a health benefit on the host. This definition includes many different microorganisms, and the potential health

benefit will depend on the specific strain, but they can be shared among the specie or the genera (Hill et al., 2014).

It has been shown that probiotics can be used to treat different illnesses such as colic and acute diarrhea, to manage the symptoms of occasional constipation and lactose intolerance, and also to prevent several afflictions such as necrotizing enterocolitis, antibiotic-associated diarrhea, atopic dermatitis or food hypersensitivity, reduce the low-density lipoprotein cholesterol related to chronic cardiovascular diseases, reduce incidence and duration of common infectious diseases in the upper respiratory tract and gastrointestinal track, extend remission of ulcerative colitis, improve therapeutic efficacy of antibiotic treatment of bacterial vaginosis, and prevent *Clostridium difficile* diarrhea (Sanders et al., 2018), among several other effects that are presented in the Figure 1.2. Possible distribution of mechanisms among probiotics (Hill et al., 2014).

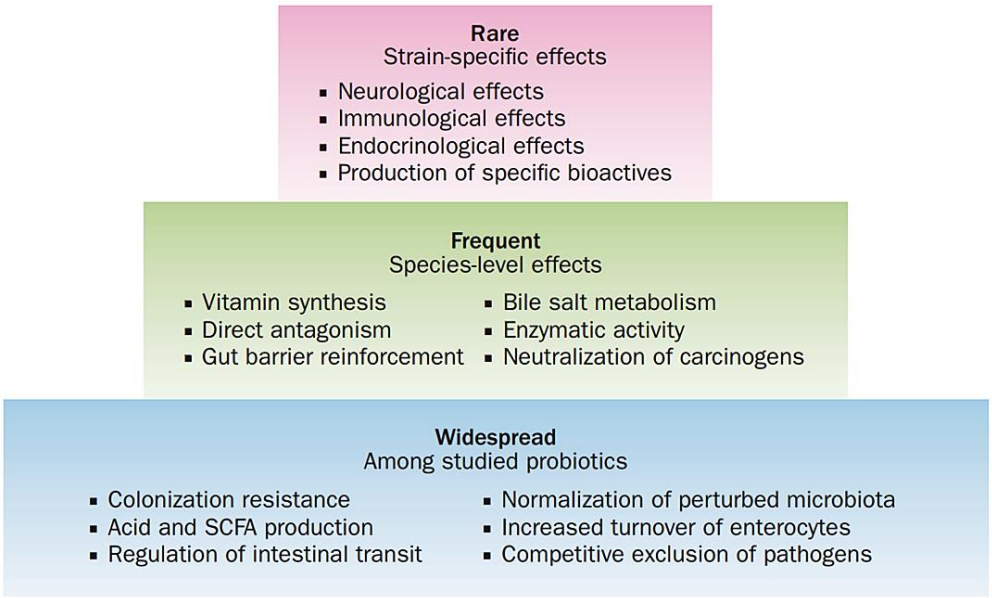

Figure 1.2. Possible distribution of mechanisms among probiotics (Hill et al., 2014).

Therefore, probiotics can be an important asset for the treatment and prevention against several illnesses. They can be found in fermented products such as dairy, but also in the form of dietary supplements. Nevertheless, for a probiotic to be effective it requires to accomplish the following characteristics: (I) to be alive when administered, (II) to have a health benefit identified in the specific strain, and (III) to be delivered at an effective dose (Hill et al., 2014). Thus, probiotic functionality is impacted by the quantity and viability of microorganisms. In this context, probiotic manufacturers require precise analytical tools to quantify the viable probiotic micro-organisms efficiently (Chiron et al., 2018).

1.3. Cell viability and functionality

Cell viability refers to the ability of a cell to grow and reproduce itself under defined environmental conditions, this definition requires that a single viable cell to be able to grow and generate a colony of cells (Kumar & Ghosh, 2019). In industrial biotechnology, cell viability is relevant during a fermentation since it can modify the quantity or the quality of a product. For example, it has been shown that cell viability can impact the quality in any recombinant protein process, using bacteria, yeast or cell line cultures (Swaminathan et al., 2022). For the use of microorganisms as probiotics, a control of the cell viability is fundamental since they are required to be alive to be considered probiotics. For this reason, several methodologies have been developed in order to measure the cell viability online and offline.

Classical microbiological techniques are efficient to determine the population of viable cells, but they can only distinguish them between viable cells and non-viable cells, meanwhile it has been shown that between these two states a cell can adopt several transition states where it loses certain characteristics of a viable cell without being dead; these cells are known as damaged cells (Oliver, 2005). Then, in order the consider a cell viable or live cell, it must accomplish certain characteristics (Díaz et al., 2010):

- Cell growth: the direct evaluation of the viability, the cell should be able to reproduce under defined conditions.

- Metabolic activity: this characteristic suggests the absence of cell death, but the measurements based on it can be inefficient to determine if a cell is alive or dead in the case of cell damage, dormancy, or starvation. This is cause by the sensitivity of the methods which could place these states under the detection limits (Díaz et al., 2010). Besides, metabolic activity can be present in a dead cell since enzymatic reactions are usually independent of other cell functions as the production of ATP. Then detecting enzymatic activity just demonstrates the presence of enzymes possibly synthetized in the past and their ability to remain active during a period of time (Wilkinson, 2018).

- Membrane potential: strictly linked to the ATP synthesis, it is usually considered as a measure of the health of a microorganism. Only live cells can maintain a membrane potential; nevertheless, membrane depolarization does not imply the death of a cell but only reduction in the cell activity (Díaz et al., 2010).

- Membrane integrity: it indicates the ability of a cell to generate gradients and hence membrane potential and enzymatic activity. Even though membrane integrity is not a guarantee of replication, damaged or compromised membrane is the definitive indicator of cell death (Díaz et al., 2010).

Damaged cells lose the previously mentioned characteristics (Figure 1.3) and can reach a state where it fails to grow on bacteriological media on which it would normally grow, but it is capable of renewed metabolic activity and regain cultivability after being cultured in a highly nutritive media in a process called resuscitation. These cells are known as viable but non-cultivable cells (VBNC) (Oliver, 2005), and this is the reason why it is necessary to evaluate not only the cell's ability to be cultured, but also the characteristics that make it viable.

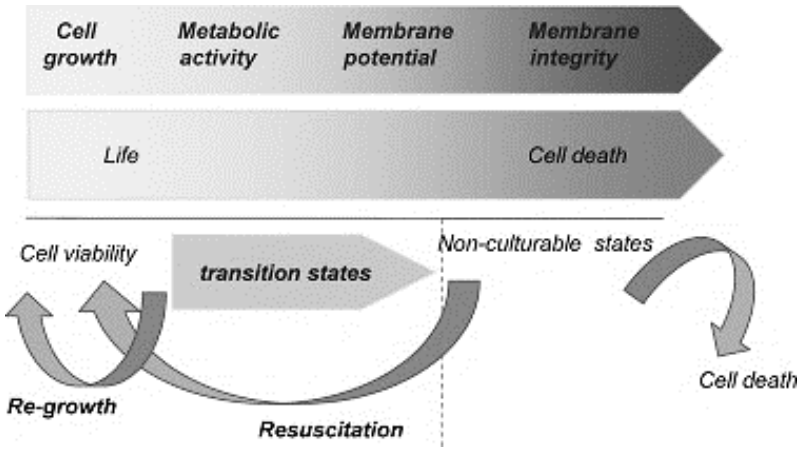

Figure 1.3. Functional criteria to determine different levels of cell viability and the different states between cell viability and cell death (Díaz et al., 2010).

1.3.1. Culture-based techniques

The gold standard of classical microbiology is the enumeration by culture-based techniques (Wendel, 2022). Viable plate counting consists in the successive dilution of a sample followed by its culture in solid media and the count of the colonies formed, which would give the colony forming units (CFU/mL or CFU/g). With these techniques, it is possible to selectively grow a targeted microorganism using specific culture media with specific pH, nutrients, or antibiotics which would inhibit the growth of not specific microorganisms (Kumar & Ghosh, 2019).

Nevertheless, selective culture can only discriminate bacteria at the level of genus (Oliver, 2005). Other disadvantages of this method are that they are offline, which means that they do not provide a direct measurement in a bioprocess, but they are time and resource consuming since the culture of bacteria may need one to five days. Furthermore, these methods have the limitation of only being able to count cultivable microorganism only, which may not be a problem for the biotechnological industry, but it can be misleading when more than one strain can be found, for example in the dairy industry (Chiron et al., 2018). Furthermore, these methods cannot be used for the enumeration of viable but non-cultivable bacteria (VBNC), since they would be classified in in the same group of the dead cells, and it does not

provide information about the damage received by the cell that does not allow it to be cultured (Oliver, 2005). To overcome this issue nonculture-based methodologies should be considered.

1.3.2. Molecular biology-based techniques

These techniques are based on the quantification of the DNA in a population with techniques such as quantitative PCR (qPCR), also called real time PCR, assuming that the DNA concentration is directly proportional to the viable cells. To distinguish viable and non-viable bacteria, these methodologies use DNA-intercalating agents such as propidium monoazide (PMA) due to its ability to bind DNA blocking the PCR (Kumar & Ghosh, 2019). These intercalating agents are not membrane permeable, so when they are applied before the cell lysis, they will block the PCR only on the cells that have a damaged membrane, applying the membrane integrity assessment, which indicates that a cell is viable only if its membrane is intact (Baymiev et al., 2020).

Another way to quantify viable cells is to use techniques that target RNA, since it is an indicator of active metabolism (Baymiev et al., 2020). However, RNA manipulation is difficult due to the short half-life and because molecular biology protocols involve several delicate steps which make them suitable for clinical and research purposes; but not for industrial production environments (Kumar & Ghosh, 2019). Furthermore, these methods are also offline and do not provide enough information regarding the viable but non-cultivable bacteria (VBNC) as they cannot differentiate damaged cells (Oliver, 2005).

1.3.3. Flow cytometry

Flow cytometry is a technology developed to measure several parameters of the cells based on light diffusion and fluorescence at the single cell level (Chiron et al., 2018). It consists in the generation of a cell suspension that then will be passed through a thin microtube where a laser beam is localized and will be used to analyze the light scattering of each individual cell. The light can be scattered in a forward direction known as forward scatter (FSC) or in an angle known as side scatter (SSC). With the information of both scatters it is possible to differentiate cells based on its size, form, and granularity, generally the forward scatter being related to the size and the side scatter related to the form and granularity of the cell (Wilkinson, 2018).

To further improve this technique and to be able to measure the cell viability, it is possible to use fluorescent stains. Viable cell cytometry is based on the collection of fluorescent signals emitted at different wavelengths from stained cells when they are excited by the laser (Wendel, 2022). Since data is collected from individual cells, it is possible to differentiate them according to the degree of uptake of the stain. The information obtained can be related to properties such as the cell membrane integrity, its functionality, the DNA base composition or even the presence of intracellular enzymes (Wilkinson, 2018). Some of the stains that can be used are presented in the Table 1.1.

Table 1.1 Some dyes used in fluorometric flow cytometry (Adapted from Díaz et al., 2010).

Cell ligand or substrate		Dye		Ex/Em*
Nucleic acids	DNA, RNA	Ethidium bromide (EB)		510/595
		Propidium iodide (PI)		536/623
		Cyanines	TO-PRO	515/533 (TO-PRO 1) 462/661 (TO-PRO 3)
			TOTO	514 /533 (TOTO 1) 642/660 (TOTO 3)
			SYTO	485-508/498-527
			SYBR	497/520 (Sybr Green)
	DNA	DAPI		350/470
		Hoechst 33342		350/461
		DRAQ5		647/700
Total protein		FITC		495/525
Lipids		Nile Red		551/636
Fluorogenic substrates		ChemChrome dyes (CY, CB, CV6)		488/520
		FDA , CFDA, CFDA/SE, CFDA-AM		492/519
		Calcein-AM		494/517
		CTC		450/630
		FUN-1		480/ 580
Intracellular pH		BCECF-AM		482/520
		SNARF-1		510–580/587–635
Membrane energization		Rh123		507/529
		$DiOC_6$ (3)		484/501
		$DiOC_2$ (3)		482/497
		$DiBAC_4$(3)		488/525
		JC-1		498,593 / 525,585
Citoplasmic Ca^{+2}		Indo-1		361,330/405, 480
Antibodies or oligonucleotides		BODIPY		503/512
		PE, PE-Cy5 conjugates		490/575, 690
		Alexa Fluor 488		495/519
		Oregon green		496/524
Autofluorescent proteins		GFP and derivatives		489/508

Different protocols that use a combination of two fluorescent stains have been developed to differentiate precisely between live, death and damaged cells using different functional criteria according to the stain choice.

- Membrane integrity criteria: some DNA stains such as SYTO 9 or SYTO 24 are membrane permeable, which allow them to mark all the dead, damaged and live cells (Wilkinson, 2018). One of these dyes is usually used with another dye usually propidium iodide (PI) which is not membrane permeable, and it can replace the SYTO dyes. In this way, the live cells are stained by the green SYTO dye and the dead cells by the propidium iodide (Díaz et al., 2010).

- Membrane potential criteria: It can be measured using charged lipophilic dyes that can cross the cell membrane and accumulate according to its charge. There are cationic dyes such as carbocyanines, DiOCn and Rhodamine; and anionic dyes such as oxonols. Ideally, the fluorescent signal is directly related to the energy levels of the cell (Díaz et al., 2010).

- Metabolic activity criteria: several metabolites are used for the determination of the metabolic activity, some of them are presented in Table 1.1Table . Esterase activity is one of the most common ways to evaluate the metabolic activity. Carboxyfluorescein diacetate (cFDA) is a dye that can pass through the cell membrane due to its neutral nature, where it can be cleaved by esterase to produce fluorescent derivates that cannot pass through the membrane (Díaz et al., 2010). Hence, the cells with intact membrane and metabolic activity will be stained, but those with damaged membrane will not retain the fluorescent compounds. This dye is often used with PI order to stain the cells with compromised membranes (Díaz et al., 2010).

1.3.4. Permittivity probes

Permittivity probes are used to evaluate the viable cell density by the membrane integrity criteria considering the dielectric properties of the cell (Metze et al., 2020). When an electrical field is applied to a material, the response from this material can be described by its conductivity (σ, in S/m) and its permittivity (ε, in F/m). The conductivity is the measure of the material ability to conduct the charges, while the permittivity is a measure of the material ability to get polarized and store the charges (Markx & Davey, 1999).

For most cell suspensions and tissues, the permittivity and the conductivity are not constant in different frequencies of alternate electrical fields. The conductivity tends to increase in steps as the frequency of the electrical field increases, but the permittivity tends to decrease. The steps of permittivity reduction are called dispersions (Figure 1.4) and each one reflects the loss of a particular polarization process increasing frequencies (Markx & Davey, 1999):

- α-dispersion (<10 kHz): this is due to the polarization by the tangential flow ions by cell surfaces (Markx & Davey, 1999).

- β-dispersion (0.4–10 MHz): produced by the polarization of cell membranes due to the Maxwell-Wagner effect which describes the formation of charges in the interface of two materials due to the different conductivity and permittivity, in this case the materials are the cytoplasm, the membrane and the outside media (Iwamoto, 2012).

- γ-dispersion (0.1–5 GHz): produced by the polarization generated by the rotation of macromolecular sidechains and bound water (Markx & Davey, 1999).

- δ-dispersion (>1 GHz): due to the polarization by the rotation of small molecules including water (Markx & Davey, 1999).

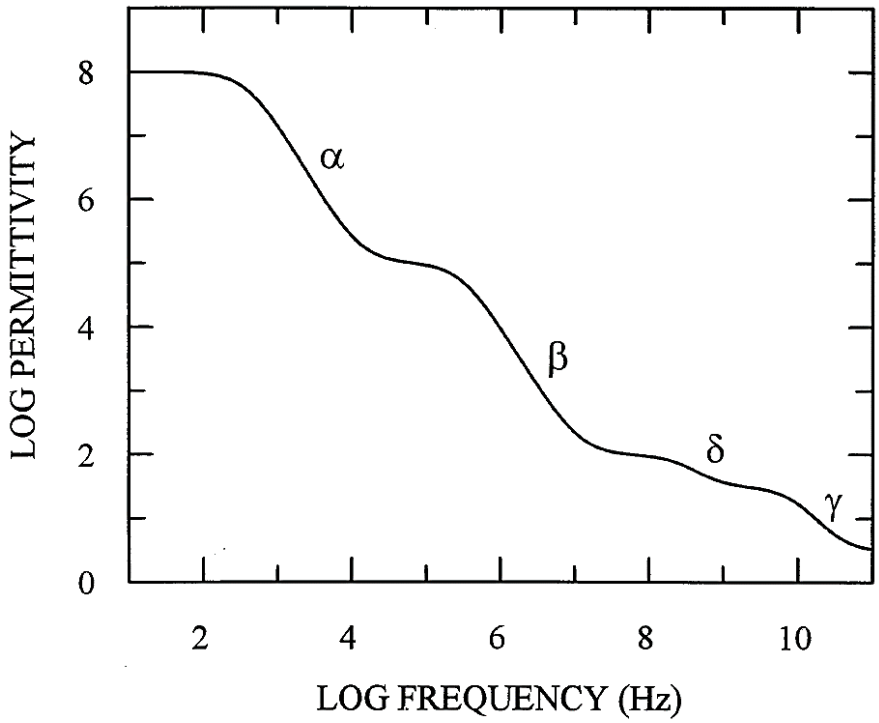

Figure 1.4 Idealized spectrum of the dielectric properties of cell suspensions and tissues (Markx & Davey, 1999).

The β-dispersion occurring theoretically between 400 kHz and 10 MHz can provide insights of the cell's viability and cell morphology. Since this dispersion accounts for the polarization of the cell membranes, the difference of the permittivity in the high frequency plateau after the dispersion (10-20 MHz) minus the permittivity in the plateau before this dispersion (300-1000 kHz) is directly correlated to the viable cells (Swaminathan et al., 2022). This measurement can differentiate between viable cells and non-viable

cells since dead cells with compromised cell membrane will not generate a polarization since the ions would leak through the damaged membrane (Metze et al., 2020).

The curve of the β-dispersion is described by the Cole-Cole equation which includes several parameters represented in Figure 1.5 that can be related to the cell morphology (Metze et al., 2020). As previously mentioned, the difference of the permittivity before and after the dispersion called relative permittivity (Δε) is directly proportional to the viable cell density (VCD) or viable cell concentration (VCC). The characteristic frequency (f_c) where the polarization rate is half completed is related to the medium cell size, a higher fc indicates a smaller size meanwhile a lower fc corresponds to a higher size. The slope (α) of the curve in the point of the characteristic frequency indicates the distribution of the cell size, a steep slope implies a homogenous cell size (Swaminathan et al., 2022).

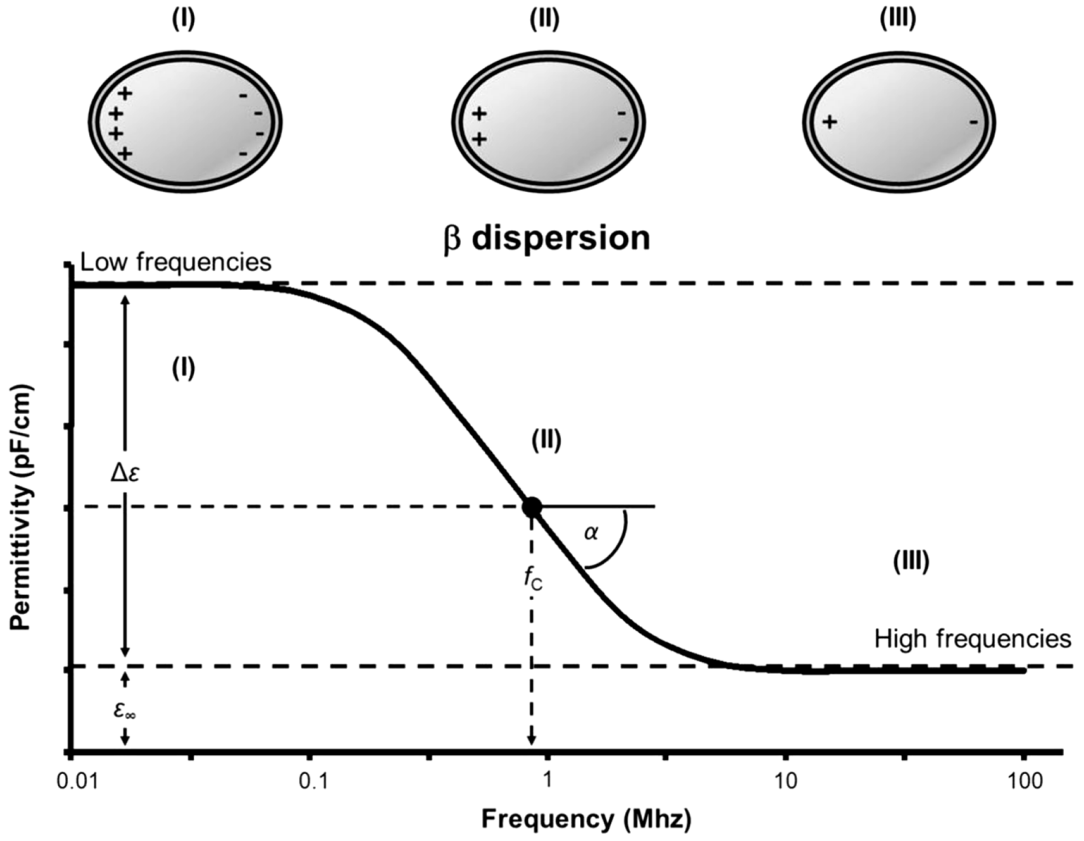

Figure 1.5 Schematic representation of the β-dispersion with the key parameters of the curve (Flores-Cosío et al., 2020).

Since the relative permittivity (Δε) is directly proportional to the viable cell density, it is possible to estimate it with the permittivity measurements. However, this relationship is strongly dependent of the cell morphology and cell content, especially the membrane composition (Metze et al., 2020). Due to this

fact, it is possible to determine a linear equation between the permittivity of the culture media and the viable cell density during the exponential phase of a specific microbial strain, in which the morphology and its dispersion in the population remains constant (Flores-Cosío et al., 2020). It is also possible to build a non-linear model to estimate the cell viability during all the phase of the cell culture, which should take into account the physiology changes by using permittivity measurements through the whole β-dispersion (Metze et al., 2020).

In another, it has been shown that the culture media capacitance can be also linearly correlated to the viable cell density during the exponential growth phase (Swaminathan et al., 2022), due to its close relationship with the permittivity presented in Eq. 1.

$$Permittivity\,(f) = Capacitance\,(f) - Capacitance\,(10\,MHz$$

Eq. 1 Relationship between the capacitance and the permittivity.

2. State of the art

Th use of permittivity probes to monitor a fermentation process presents several advantages against in-line monitoring technologies such as turbidity or pH, and off-line monitoring such as flow cytometry or molecular techniques (Flores-Cosío et al., 2020):

- The permittivity probes are sterilizable.
- The measure is on-line, allowing to know the state of the culture in real time.
- It is applicable to high density fermentations.
- It is a non-destructive method.
- It only detects viable cells based on the membrane integrity criteria.

Nevertheless, this technology has some drawbacks that should be considered when they are implemented. The main one is that a change in the physiological state of the cells would change the correlation between permittivity and viable cell density (Bergin et al., 2022). Despite the possibility of using this information to evaluate the cell physiology, it increases the complexity of its application for microbiological cultures (Flores-Cosío et al., 2020).

2.1. Permittivity probes use in cell culture

The application of the dielectric studies in the microbiology dates to the decade of 1900s when it was demonstrated the existence of the cellular membrane based on electrical properties, but it is in the last few decades that the application of this technology for monitoring cell culture became more frequent (Justice et al., 2011). The main application of this technology is in the culture of cell lines, mainly but not limited to mammal cells.

Permittivity probes have been used successfully monitoring cell concentration, cell viability, and physiological state changes in Chinese hamster ovary (CHO) cells using batch and fed-batch strategy; in airlift, stirred and wave bioreactor (Bergin et al., 2022; Metze et al., 2020). The permittivity probes have been applied successfully also to human cells lines such as HeLa, plant cell lines, and insects cell lines (Bergin et al., 2022). These examples range from lab scale to production scale, and include the production of recombinant proteins, viruses, and antibodies (Justice et al., 2011).

The use of permittivity probes has been successful for cell lines since they have homogenous shapes and sizes which allow the easy determination in physiological state, detection of apoptosis, and the correlation of permittivity and viable cell density (Justice et al., 2011). Meanwhile, its adaptation to microbial cell cultures has been slower (Flores-Cosío et al., 2020).

2.2. Application of permittivity probes for bacterial and yeast fermentations.

The main use of permittivity probes is the measurement of the cell growth, concentration, and viability in-line, but it is not limited to it. The monitoring has been reported for several yeast such as *Saccharomyces cerevisiae, Pichia pastoris* and *Kluyveromyces marxianus;* for gram-positive bacteria such as *Bacillus megaterium* and gram- negative bacteria like *Escherichia coli*; and for filamentous fungi. This application has also been reported for batch and fed-batch culture (Flores-Cosío et al., 2020).

Knabben (2011) demonstrated the linear correlation between the permittivity measure and the offline measurements of biomass concentration in high cell density cultivation of *Escherichia coli* using a fed batch strategy. The biomass concentration was determined by dry cell weight and the linear correlation was proven for the cells maintained in exponential phase for cell concentrations up to 90 grams per liter. In another study (Swaminathan et al., 2022), it was demonstrated the linear correlation between the permittivity and the viable cell density during the exponential phase, but also a non-linear model was produced and validated to determine the viable cell density, the total biomass, and the cell diameter using the Cole-Cole model, online and offline data.

The permittivity measures have also been applied to determine morphological changes such as size and form. Another application is the detection of physiological states or growth phases which have been applied in organisms such as *Bacillus thuringiensis* (Flores-Cosío et al., 2020). Permittivity measurement have been useful even to detect the formation of lipid droplets intracellularly in *Arxula adeninivorans* (Flores-Cosío et al., 2020).

Despite the high potential of permittivity probes, they present some drawbacks when applied. In microorganisms not studied previously, it is necessary to apply several off-line methods to correlate the permittivity results to the physiological state; the lack of this information may lead to difficulties or misinterpretation of the data obtained (Flores-Cosío et al., 2020; Swaminathan et al., 2022). Even more, as this technique relies on the cell membrane integrity criteria to measure the cell viability, it is not capable of measuring the loss of viability due to biotic and abiotic factors that do not affect the membrane (Justice et al., 2011). Finally, this technique is affected by changes in morphology, cell size, and intracellular concentration of metabolites, which makes more important the previous study of the cell physiology using off-line methods (Flores-Cosío et al., 2020).

2.3. *Bifidobacterium animalis subsp. lactis*

Bifidobacterium is a genus of lactic acid producing, non-spore forming, Gram-positive, non-motile, anaerobic bacteria. *Bifidobacterium animalis* subsp. *lactis* is a catalase-negative, rod-shaped bacterium. It shows low tolerance to oxygen and it grows optimally at pH of 6, but it resist pH as low as 2. (Jungersen et al., 2014). It is one of the most common *Bifidobacterium* species and it has been utilized as a probiotic and applied in fermented foods for decades (Uusitupa et al., 2020).

Several health benefits have been attributed to this microorganism and several treatments featuring it are under clinical trials. It has been shown that *B. lactis* has the characteristics needed to become part of the microbiota after ingestion such as acid resistance, bile salt resistance through enzymatic hydrolysis, and mucus adhesion (Jungersen et al., 2014). *In vitro* and *in vivo* studies in mice have shown that this bacterium can maintain a healthy gut microbiota by delaying the aging process and by competing and excluding harmful pathogens. It has been also proposed that it can stimulate the immunological system and maintain the epithelium integrity which contributes to a healthy gut (Cheng et al., 2021).

It is demonstrated that *B. lactis* stimulates the bowel motility reducing constipation, it prevents diarrhea in children and antibiotic-associated diarrhea (Jungersen et al., 2014). Some clinical trials have focused on the use of this microorganism in the prevention and treatment of respiratory track diseases and oral diseases (Araujo et al., 2022). Some studies suggest that *B. lactis* ingestion reduces the fat mass gain in obese and diabetic mice, reduce the hyperglycemia, increase the insulin sensitivity and reduce the risk of cardiovascular diseases (Uusitupa et al., 2020).

2.4. *Lactobacillus acidophilus*

Lactobacillus acidophilus is a Gram-positive, rod-shaped bacterium that grows optimally in temperatures between 37°C and 42 °C, and in slightly acid media with pH between 5.5 and 6.0, but it can grow in temperatures as high as 45°C and in pH as low as 4.0. It is an obligated anaerobic bacterium being one of the least oxygen tolerant of the lactobacilli. As it is an obligated homofermentative, it produces lactic acid by the fermentation of carbohydrates (Bull et al., 2013). Genomic analyses have determined that *L. acidophilus* is auxotrophic for 14 aminoacids and it is unable to produce multiple cofactors such as biotin, nicotinamide, folate, riboflavin, and pyridoxine. This explains its need to growth in nutrient rich media (Bull et al., 2013).

This strain was first isolated from infant feces, it has been determined that it populates the gastrointestinal track and that it can be also located in the environment as part of plant and animal microbiota. *In vivo* studies have found that it displays resistance to low pH and bile salts, adhesion to human colon cells in

cell culture, antibiotic production, and lactase activity, important characteristics for gastrointestinal track probiotic bacteria (Gao et al., 2022).

Several probiotic effects have been attributed to strains of *L acidophilus*, some of them are the improvement in lactose intolerance thanks to the production of lactase, the inhibition of the development of intestinal diseases and enhance immunity due to the induction of anti-inflammatory response and modulation of the immune response, prevention and treatment of colon cancer, the inhibition of cardiovascular diseases progression, and the prevention of hepatocarcinogenesis, besides regulation of the intestinal microbiota (Gao et al., 2022).

Industrially, it possesses the GRAS status with the FDA, and it is part of several undefined starter cultures for fermented products. It can be found in milk, yogurt, toddler formula and other fermented products. Considering that *L. acidophilus* grows slowly in milk products, this microorganism is usually added after the main fermentation to increase its probiotic value (Bull et al., 2013; Shah, 2000).

3. Objectives

3.1. General

This project objective is to apply the measurement of capacitance and permittivity to estimate the viable cell density in 1-liter 24-hours batch cultures of bacterial models of industrial interest: *Bifidobacterium animalis* subsp. *lactis, Lactobacillus acidophilus*.

3.2. Particular

- Determine the kinetics of acidification, optical density, carbon source consumption, and cell viability by viable cell count and flux cytometry in 1-liter batch cultures of the mentioned bacterial strains.
- Measure the culture media capacitance during the fermentations at different frequencies, from 300 kHz to 10 MHZ and determine the permittivity for it at 580kHz.
- Correlate viable cell density measurements with the permittivity measurements during the exponential phase of growth by a linear model.
- Assemble a non-linear model that correlates the viable cell density and the capacitance measurements during all the measurement phases using the available software.
- Implement the model for regular use in the laboratory.

4. Materials and methods

4.1. Strains and culture media

The experiments were performed using the strains *Bifidobacterium animalis* subsp. *lactis* DSMZ 10140, *Lactobacillus acidophilus* ATCC 4356. The lactic strains were maintained at -80°C in aliquots of 50% v/v seed culture, 30% v/v glycerol, and 20% v/v of a sterile solution of 110 g/L non-fat dry milk (ITW Reagents).

4.1.1. Seed culture

The seed culture was performed in 500 mL bioreactor (Getinge, Applikon) equipped with pH and temperature probes, or in 60 mL T-flasks. The working volume was 400 mL culture media for the bioreactor and 60 mL for the T-flasks. The culture media was BSM broth (Bifidum Selective Media, Sigma Aldrich) supplemented with 0.5 g/L of sodium ascorbate for *B. lactis*, and MRS broth (DeMan, Rogosa and Sharpe, Becton, Dickinson, and Company) for *L. acidophilus*. The inoculation was performed with 2% v/v of initial aliquot and the culture was performed for 20-24 hours at 37°C and with a stirring speed of 100 rpm. The pH probe was calibrated before every experiment.

Unstained microscopic observations and optical density measurements were performed at the end of every seed culture to verify the morphology and the purity of the strain.

4.1.2. Main culture

The main culture was performed in a set of four 1-Liter bioreactors (Multifors 2, Infors HT) equipped with temperature, pH, and permittivity probes. The culture was monitored and controlled through the software Eve (version 2021 H1) proportionated by the bioreactor's manufacturer.

The culture media for each microorganism was prepared to attain the concentrations presented in Table 4.1. To avoid undesired reactions or decomposition of the ingredients, they were sterilized separately. The magnesium sulphate, manganese sulphate, and the cysteine were sterilized by 0.2 µm microfiltration of concentrated solutions (20%, 10% and 20% w/v respectively). The yeast extract was sterilized in the autoclave (121°C for 15 minutes) in a solution in double concentration. Another solution in double concentration of the rest of the components was sterilized in the same conditions. At the end, the culture media was assembled with the correct volume of each solution to achieve the concentrations presented in Table 4.1.

Table 4.1 Culture media composition for the main culture of *B. lactis* and *L. acidophilus*.

	B. animalis subsp. lactis		***L. acidophilus***	
Sterilization method	Component	Concentration (g/L)	Component	Concentration (g/L)
Autoclave (15 min @ 121°C)	Procelys Yeast Extract 1	20	Procelys Yeast Extract 2	20
Separately in autoclave (15 min @ 121°C)	Glucose ($C_6H_{12}O_6$)	40	Glucose ($C_6H_{12}O_6$)	40
	Sodium ascorbate ($NaC_6H_7O_6$)	0.5	Sodium ascorbate ($NaC_6H_7O_6$)	0.25
	Sodium chloride (NaCl)	5	Sodium acetate ($NaCH_3CO_2$)	1
	Calcium chloride ($CaCl_2$)	0.01	Ammonium citrate dibasic ($C_6H_{14}N_2O_7$)	0.5
	Sodium bicarbonate ($NaHCO_3$)	0.4	Potassium phosphate dibasic (K_2HPO_4)	2.5
	Potassium phosphate dibasic (K_2HPO_4)	0.05	Potassium phosphate monobasic (KH_2PO_4)	1.25
	Potassium phosphate monobasic (KH_2PO_4)	0.05	Tween 80	1
	Tween 80	1		
Microfiltration (0.2 µm)	Magnesium sulfate ($MgSO_4$)	0.2	Magnesium sulfate ($MgSO_4$)	0.2
	Manganese sulphate ($MnSO_4$)	0.05	Manganese sulphate ($MnSO_4$)	0.1
	Cysteine	0.5		

For *B. lactis*, the pH of the culture media was adjusted to 6.5 before the inoculation and it was regulated to a minimum of 6.0 by the automatic addition of a concentrated solution of sodium hydroxide (NaOH 25% w/v) during the fermentation. For *L. acidophilus*, the pH of the culture media was adjusted to 6.4 before the inoculation and it was regulated to a minimum of 5.5 with ammonium hydroxide (NH_4OH 15% w/v).

The bioreactor was inoculated with 20 mL of the seed culture (2 % v/v) from the seed culture bioreactor or the T-flask after 20-24 hours of incubation. The bioreactor was maintained at a temperature of 37°C and at an agitation of 100 rpm during the fermentation.

Samples of 10 mL were taken from the bioreactor for the offline analysis every two to three hours. To collect these samples during the 24 hours of fermentation, 4 bioreactors were launched for each biological replicate. These bioreactors were inoculated with the same seed culture with delayed start of 5 hours each. To delay the start of the culture, the temperature was fixed at 10 °C during the waiting time.

The pH probe, the base regulation pump and the seed culture feed pump were calibrated before every experiment.

4.2. Online capacitance measurements

Capacitance measurements were conducted with a permittivity probe (Hamilton, Incyte Arc 12 mm diameter) which have four offset, platinum electrodes inclined in the same direction as the probe body. The measurements were performed in frequency scan mode which collects the capacitance measurements from 300 kHz to 10 MHz in every sampling time and calculates the permittivity of a determined frequency.

4.3. Offline viable cell density measurements

4.3.1. Viable cell count

The device easySpiral Dilute (Interscience) was used to automatically make tenfold serial dilutions of a sample and inoculate the final dilution in agar plates. The inoculation and the colony count were performed according to the recommendation of the manufacturer to obtain the colony forming units per milliliter (CFU/mL). The measurements were performed in triplicate.

For the count of *B. lactis*, commercial BSM agar (Sigma-Aldrich) supplemented with 0.5 g/L of sodium ascorbate was used. Once inoculated, the plates were incubated at 37°C for 48 hours inside an anaerobic box. For *L. acidophilus*, commercial MRS agar (Difco, BD Diagnostics) was used. Once inoculated, the plates were incubated at 37°C for 24 hours inside an anaerobic box.

4.3.2. Flow cytometry

Flow cytometry was used in this study to quantify the cells with specific viability properties. The double stain methodology allowed for the discrimination of live, damaged, and dead cells. In both protocols, the samples were diluted in tenfold serial dilution to the correct one and the reagents were added using the

robot OT-2 (Opentrons) with PBS solution (Phosphate-buffered saline solution; 137 mM NaCl, 10 mM phosphate, 2.7 mM KCl; pH~7.4). The analyses were carried out in the flow cytometer CyFlow Space (Sysmex Partec) equipped with an autoloader.

Before and after every manipulation the equipment was cleaned with decontaminating solution, cleaning solution and bleach according to the manufacturer recommendations. Two methodologies were applied, one with the use of propidium iodide (PI) and Syto 24 as fluorochromes to evaluate the samples by the membrane integrity criteria, and another one with the use of cFDA and PI to use the metabolic activity criteria.

Prior to analysis, samples were serially diluted to a concentration where the device could measure between 500 and 5000 signals per second at flow rate of 2 microliters per second. To prepare them, 200 µL of the diluted sample was placed in a microplate well, in which two microliters of the first fluorochrome was added and mixed, then the sample was incubated in 37°C for 15 minutes, and this process was repeated for the second fluorochrome. For the methodology S24/PI, propidium iodide at an initial concentration of 0.2 mM was first followed by the Syto 24 at a concentration of 0,1 mM. For the methodology cFDA/PI, the cFDA at a concentration of 10 mM was added first followed by the PI at a concentration of 1.5 mM.

For each microbial strain before the sample analysis, a calibration was performed. A sample from the experiment is used to represent the live cells, even though the viability is not 100%. To represent the dead cells, the experiment sample is used but it is incubated in boiling water for 15 minutes to kill the cells.

For the methodology S24/IP, the samples were prepared according to the Table 4.2. The standard was used to determine the electronic gains for the FSC and SSC detection and the creation of gates that differentiate the cell signals from the noise signals; the rest of the samples were used to create gates that would differentiate between live, damaged, and dead cells.

Table 4.2 Samples for the flow cytometry calibration with the method Syto24/PI

Sample	Live cells (mL)	Dead cells (mL)	PI 0.2 mM (µL)	Syto 24 0.1 mM (µL)
Standard	2	0	0	0
100% alive	2	0	20	20
75% alive	1.5	0.5	20	20
50% alive	1	1	20	20
25% alive	0.5	1.5	20	20
0% alive	0	2	20	20

For the methodology cFDA/PI, the samples for the calibration were prepare accordingly to the Table 4.3, the standard had the same function as the previous method, the other two samples were used to setup the gates and the electronical compensation to differentiate between active and inactive cells. This electronic compensation has the objective of electronically reduce the red signal obtained from the large emission spectrum of the fluoresceine that interferes with the red signal which correspond to the propidium iodide.

Table 4.3 Samples for the flow cytometry calibration with the method cFDA/PI

Sample	Live cells (mL)	Dead cells (mL)	cFDA 10 mM (µL)	PI 1.5 mM (µL)
Standard	2	0	0	0
100% alive	2	0	20	0
0% alive	0	2	0	20

The results of this measurements are reported as concentration of Active Fluorescent Units (AFU/mL)

4.4. Other measurements

4.4.1. Optical density

Optical density was measured with the appropriate serial dilution in the spectrophotometer at 600 nm for each sample.

4.4.2. Microscopic observations

For each sample, the unstained microscopic observations were carried out by placing a drop of the sample in a slide and placing a cover slip on top. The samples were observed in the microscope (ZEISS Axio) under a 100x immersion objective (A-Plan, 1.25 oil) and with a 10x amplification in the ocular lenses.

4.4.3. Monosaccharides and organic acids quantification

The concentration of glucose, fructose, saccharose, acetate and lactose were measured by HPLC.

4.4.4. Final wet biomass

At the end of the fermentation, 350 mL of the culture media suspension were centrifugated, the supernatant was discarded, and the pellet was weighted. This measurement was performed in duplicate.

4.5. Correlation between viable cell density and permittivity

The non-linear model was created with the software provided by the permittivity probe's producer, AirArc Data modeling (version 2021.08.2429.10, Hamilton). A minimum of four valid biological replicates were used to create the models. The obtained model is composed by a matrix of coefficients that would multiply the matrix of capacitance measurements to obtain a matrix of viable cell density at each measurement time:

$$\begin{bmatrix} a^{300kHz} & a^{374kHz} & a^{476kHz} & \cdots & a^{10MHz} \end{bmatrix} \begin{bmatrix} c_0^{300kHz} & c_1^{300kHz} & c_2^{300kHz} & \cdots & c_n^{300kHz} \\ c_0^{374kHz} & c_1^{374kHz} & c_2^{374kHz} & \cdots & c_n^{374kHz} \\ c_0^{476kHz} & c_1^{476kHz} & c_2^{476kHz} & \cdots & c_n^{476kHz} \\ \vdots & \vdots & \vdots & \ddots & \vdots \\ c_0^{10MHz} & c_1^{10MHz} & c_2^{10MHz} & \cdots & c_n^{10MHz} \end{bmatrix} = \begin{bmatrix} VCD_0 \\ VCD_1 \\ VCD_2 \\ \vdots \\ VCD_n \end{bmatrix}$$

Eq. 2 Matrix equation that explains the calculation of the viable cell density using the model and the capacitance measurements. a^f is a coefficient of the model for the frequency f, c_t^f is the capacitance measured at the time t at the frequency f, and VCD_t is the viable cell density at the time t.

5. Results

5.1. Bifidobacterium animalis subsp. lactis

5.1.1. Kinetic study of the growth and acidification of *B. lactis*

Bioreactor runs were carried out for 24 hours. Samples were taken regularly every two to three hours. To ensure a reliable performance of the model that correlates the viable cell density and the permittivity, the fabricant of the probes recommend 4 biological replicates as a minimum, so 4 runs of the experiment were performed, and the results are presented as an average. The results of the viable cell density determination by viable cell count and flow cytometry with double staining are presented in Figure 5.1. The viable cell count represents the quantity of cells, or group of cells capable of growing in the specific solid media (BSM) and forming a colony, meanwhile the flow cytometry results correspond to the number of cells with intact membranes for the methodology S24/PI, and the number of cells with active metabolism for the method cFDA/PI.

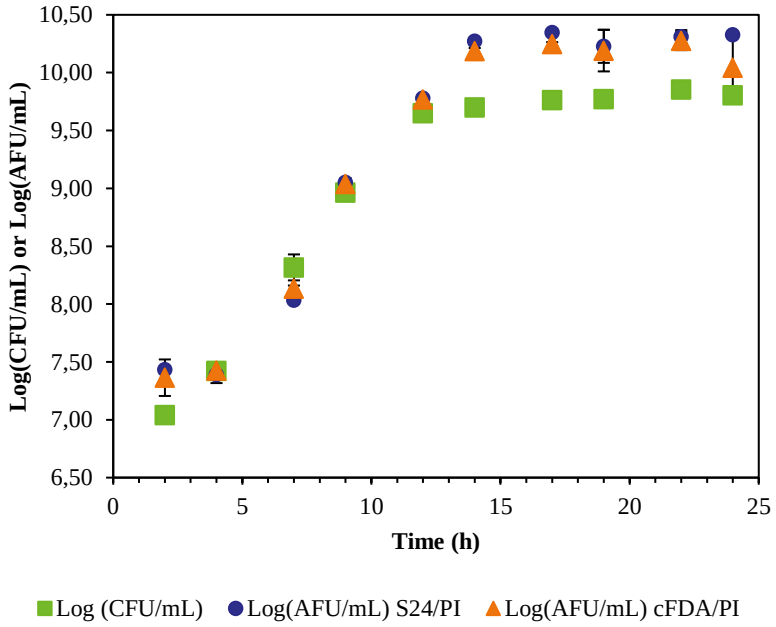

Figure 5.1 Offline measurements for Viable Cell Density of a 1-Liter batch culture of *B. lactis*. Viable cell density measured in the logarithm Colony Forming Units (CFU/mL) and Active Fluorescent Units (AFU/mL) with the methodology of double stain using Syto 24/PI and cFDA/PI.

The exponential growth phase or *B. lactis* is located between 4 and 12 hours of culture for the three determinations of viable cell density, but if we consider only the CFU/mL measurement it starts since the 2 hours of culture, and for both flow cytometry methods it extends to the 14 hours of culture. Possibly, since the beginning of the fermentation, some of the cells are in a viable but non-cultivable state, and during the lag phase which occurs from the 0 to the 4 hours of culture, the cells number do not increase

but they regain the ability to grow in that specific media. The same could happen at the end of the exponential phase, when the cells continue to multiply, but most of the cells lose their ability to grow in the solid media. This hypothesis is in line with the results of cell density presented in Figure 5.2, where the exponential growth phase prolongates from 4 to 14 hours of culture. Nevertheless, further studies are necessary to determine the factors that make *B. lactis* enter the viable but non-cultivable state.

The stationary phase starts after 14 hours of culture and the decline phase may start at 22 hours since afterwards the cell metabolic activity is affected, while the membrane integrity and the ability to grow in solid media are not.

The microbial growth of the bacteria was measured also by the optical density at 600 nm. In this measurement, the exponential phase was extended up to the 18 hours of culture as presented in Figure 5.2, meanwhile it only extended to 14 hours in the viable cell density measurements. This can be explained by the morphological changes originated during the stationary phase at the end of the exponential phase. The size of the cells tends to increase during this phase and morphological changes also occur, as the *Bifidobacterium* species are now by the "Y" shape that they take (Jungersen et al., 2014).

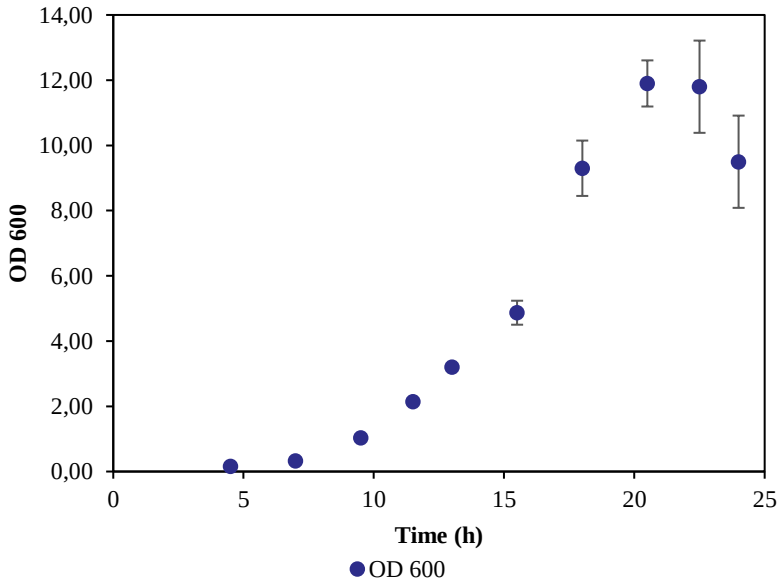

Figure 5.2 Optical density at 600 nm of *B. lactis* growth in 1-liter batch culture.

The sugar consumption, and the acetate and lactate production during the fermentation are presented in Figure 5.3. Besides culture media pH, conductivity ad the base pumped to it were also measured and the results are presented in Figure 5.5. Firstly, the concentration of glucose measured before the inoculation and the glucose added did not correspond, there is a reduction of 22,3% of the glucose during the sterilization, this is due to the high temperature of the process that converts the glucose in other

derivatives that are detected in the HPLC as fructose and trehalose and are not metabolized by the bacteria as presented in Figure 5.3.

The glucose is consumed accordingly to the growth kinetics, having a fast consumption rate between the 7 and 16 hours of culture, followed by a period of glucose consumption without microbial multiplication but with increase in the optical density of the culture and possible increase in the size of the cells. until reaching a minimum attained after 20 hours of culture. The depletion of glucose may also explain the reduction of the AFU/mL cFDA/PI after 24 hours of cultures. The production of acetate and lactate follow the same kinetic as the glucose consumption since they are coupled, reaching a maximum by the end of the fermentation, corresponding to the glucose depletion.

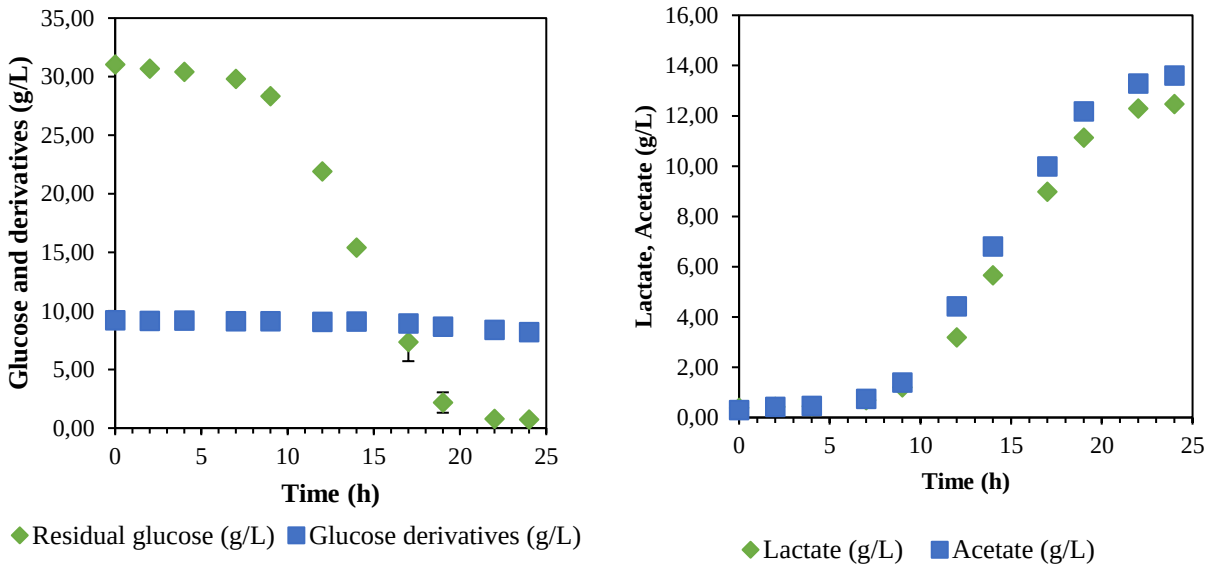

Figure 5.3 Kinetics of glucose consumption (left), and acetate and lactate production (right) of a 1-Liter batch culture of *B. lactis*.

The curves of pH, base injected and conductivity are presented are presented in Figure 5.5. The culture media reduce its pH during the first 5 hours then it is stabilized at 6 thanks to the automatic addition of base. This addition increases exponentially during the next five hours, followed by a high injection from the 10 to the 20 hours of culture. At the last 4 hours of culture the base injection is reduced. As expected, this pattern resembles the glucose consumption and acids production curves.

The conductivity follows a kinetic behavior comparable to the base addition, since the acids produced by the microorganism and the sodium hydroxide added to neutralized them are the ions that drive the increase in the conductivity.

The microscopic observations are presented in Figure 5.4 as a reference of the morphology and relative cell size.

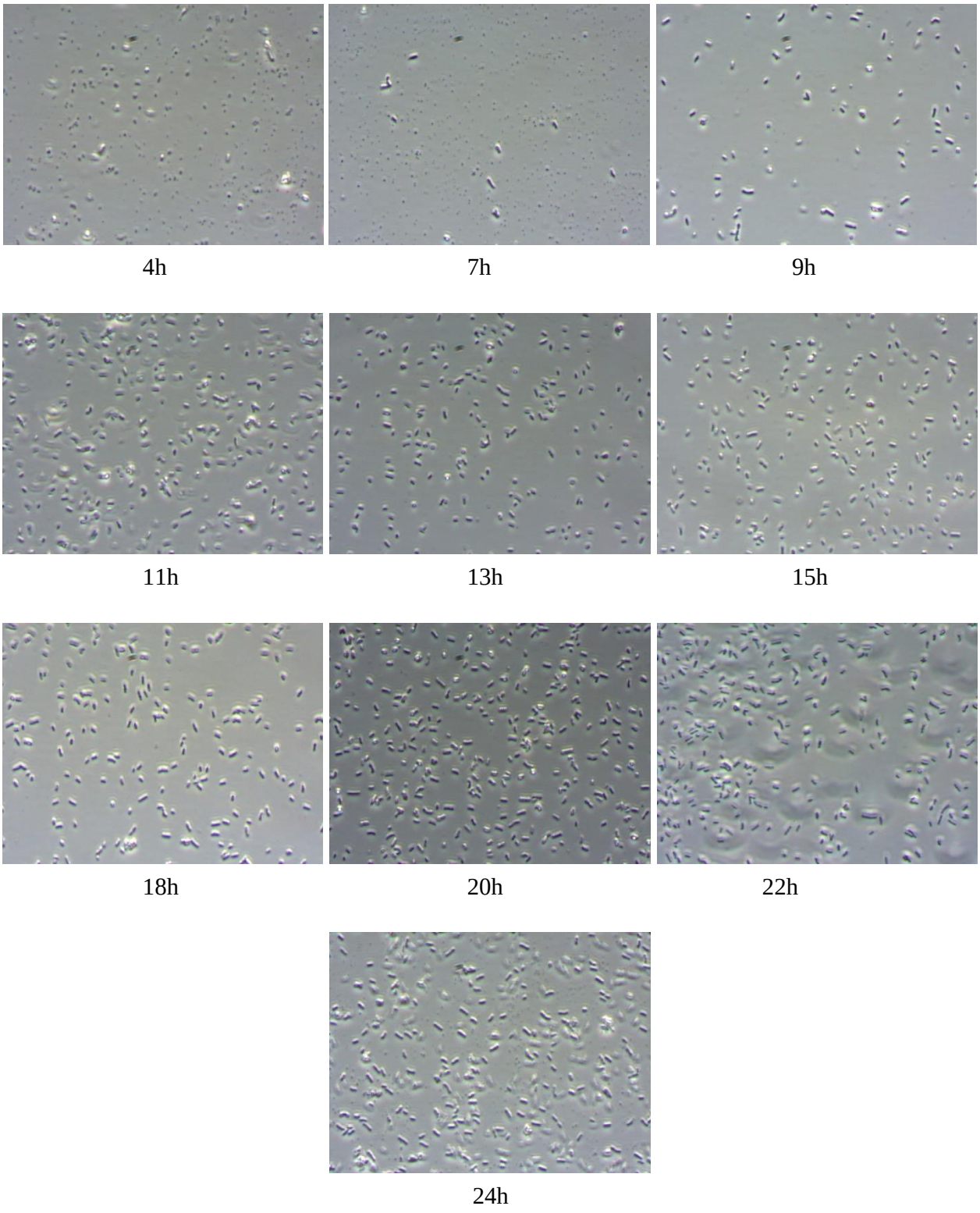

Figure 5.4 Microscopic observations of samples taken from a culture of *B. lactis* growing in mineral media with glucose as carbon source and yeast extract as a nitrogen source.

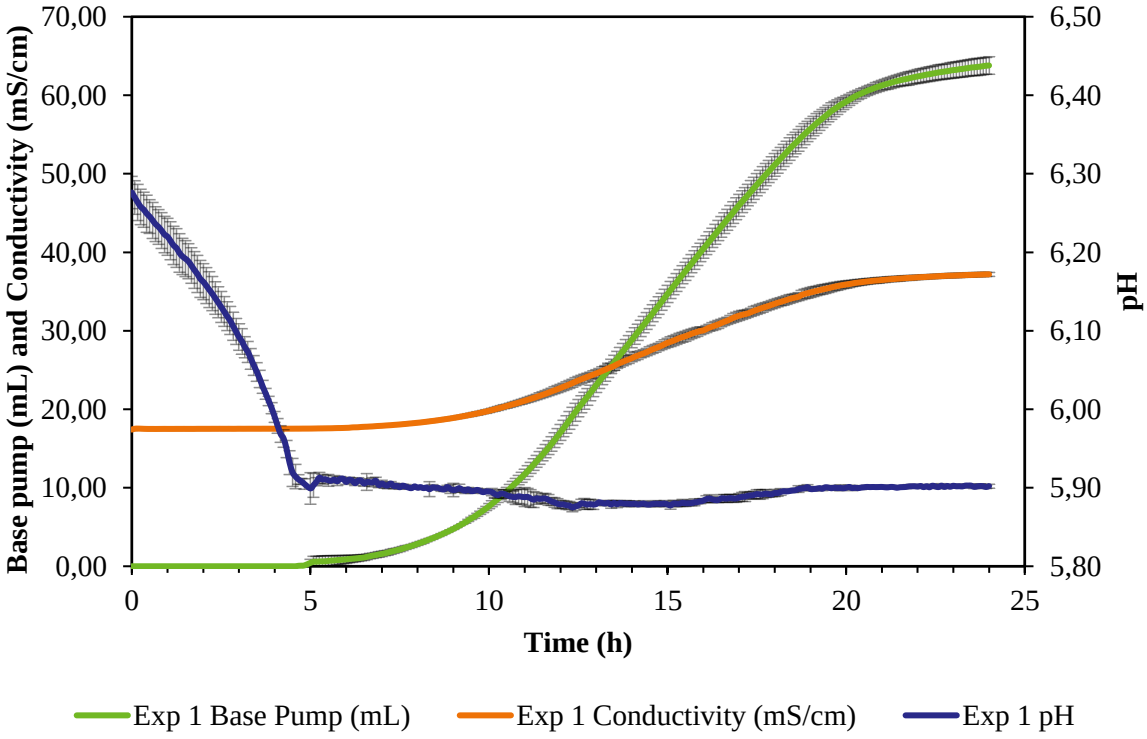

Figure 5.5 Curves of pH, injected base, and conductivity of a 1-liter batch fermentation of *B. lactis*.

5.1.2. Permittivity measurements

The permittivity at 580 kHz and the capacitance at different frequencies from 300 kHz to 10 MHz were obtained from the permittivity probes in each biological replicate. The permittivity curves of 4 biological replicates are presented in Figure 5.6, where we can notice the inconsistency in the measurements from one replicate to another, since they follow a similar tendency, but the values obtained are quite different. This inaccuracy is unique when comparing these results to the rest of the measurements (Viable cell density, OD, conductivity, pH, base injected, and glucose consumption) that were repeatable.

Besides, it has been proved that the permittivity correlates linearly with the viable cell density during the exponential phase since the morphology of the bacteria does not change significantly (Flores-Cosío et al., 2020; Siano, 1997), but in this case the permittivity did not follow this behavior during the exponential phase that prolongates from 4 hours to 12 hours of culture.

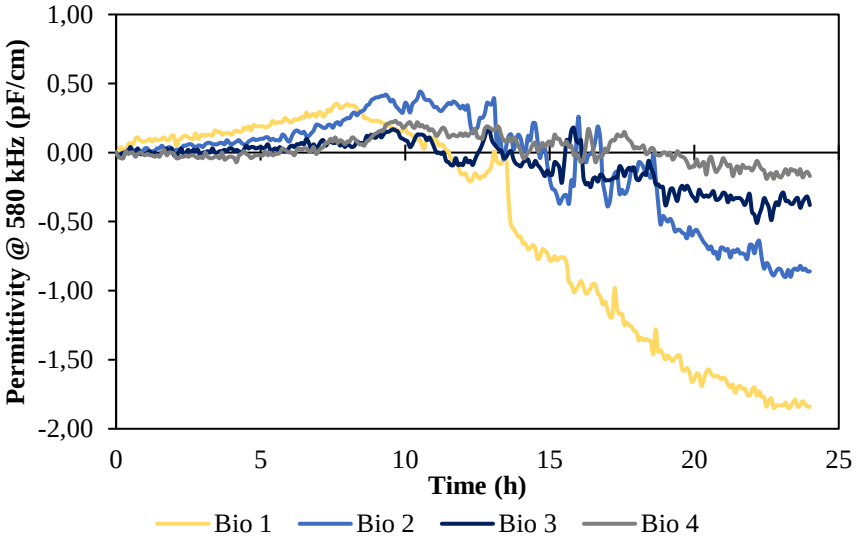

Figure 5.6 Permittivity curves measured at 580 kHz of 4 replicates of 1-liter batch fermentation of *B. lactis*.

Likewise, it has been shown that the capacitance of the culture media also can be linearly correlated to the viable cell density (Swaminathan et al., 2022). The culture media capacitance at 300 kHz is presented in Figure 5.7, where the kinetic behavior of 3 out of 4 biological replicates was similar but still with high variability. The fourth replicate did not follow the same behavior. The linear correlation during the exponential phase between the viable cell density and the capacitance at 580 kHz was evaluated for each biological replicate and for each viable cell density measurement, the results are presented in Figure 5.8. A good correlation (R^2>0.9) was found for three of the replicates for each measurement of viable cell density.

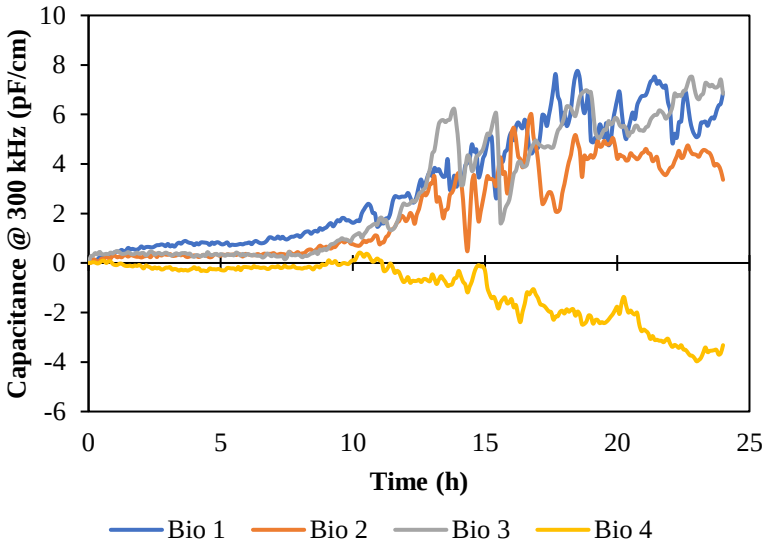

Figure 5.7 Culture media capacitance curves measured at 300 kHz of 4 replicates of 1-liter batch fermentation of *B. lactis*.

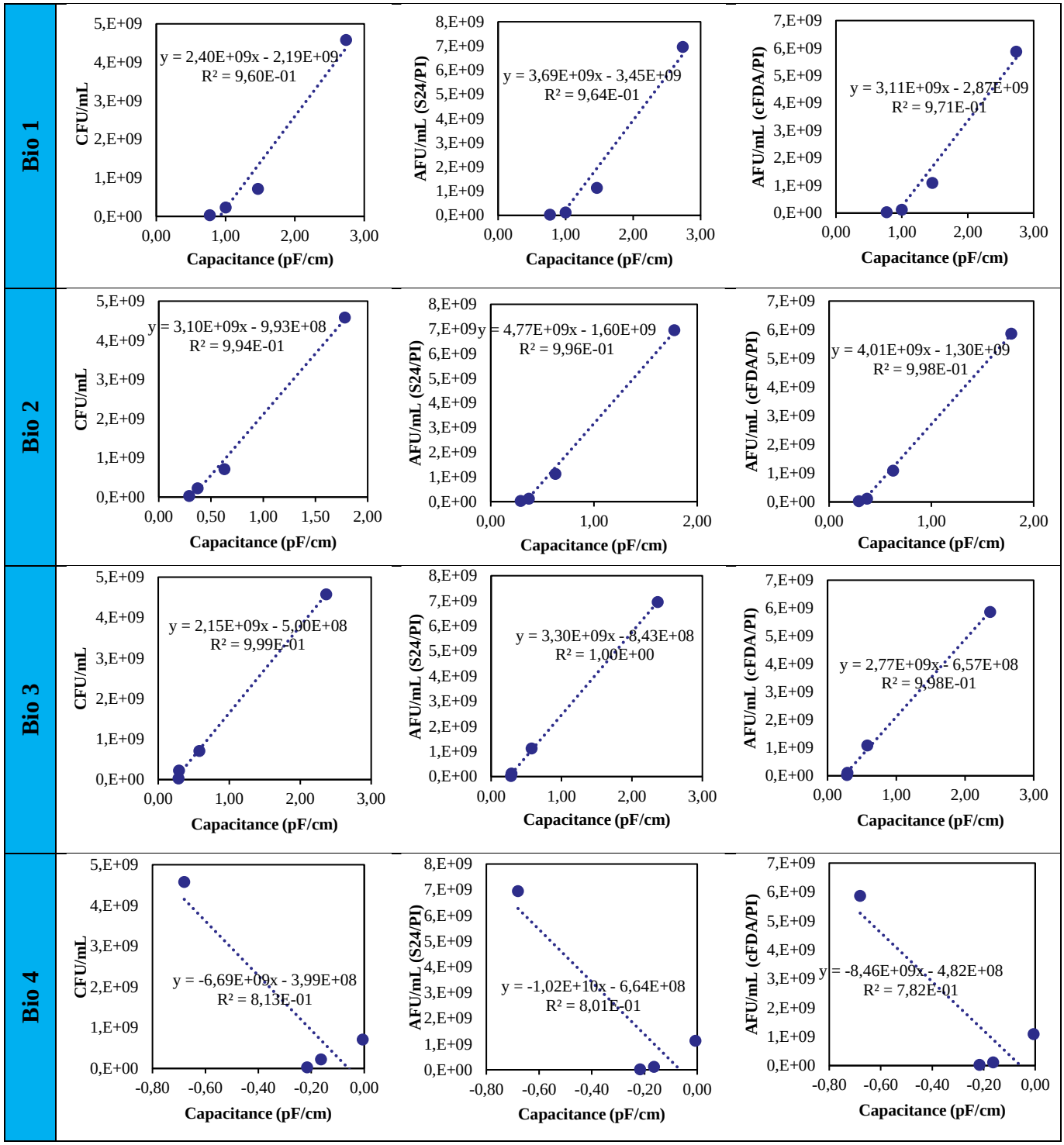

Figure 5.8 Linear correlation during the exponential phase of capacitance measurements at 300 kHz and offline measurements of viable cell density in Colony Forming Units (CFU/mL), and Active Fluorescent Units (AFU/mL) with the methodology of double stain using Syto 24/PI and cFDA/PI. Applied to 4 biological replicates of 1-liter batch fermentation of *B. lactis*.

Despite the good linear correlation obtained for each batch individually, it was not possible to stablish a good linear correlation when all the points of the three replicates were evaluated together, as it is presented in Figure 5.9, since the dispersion of the points was high.

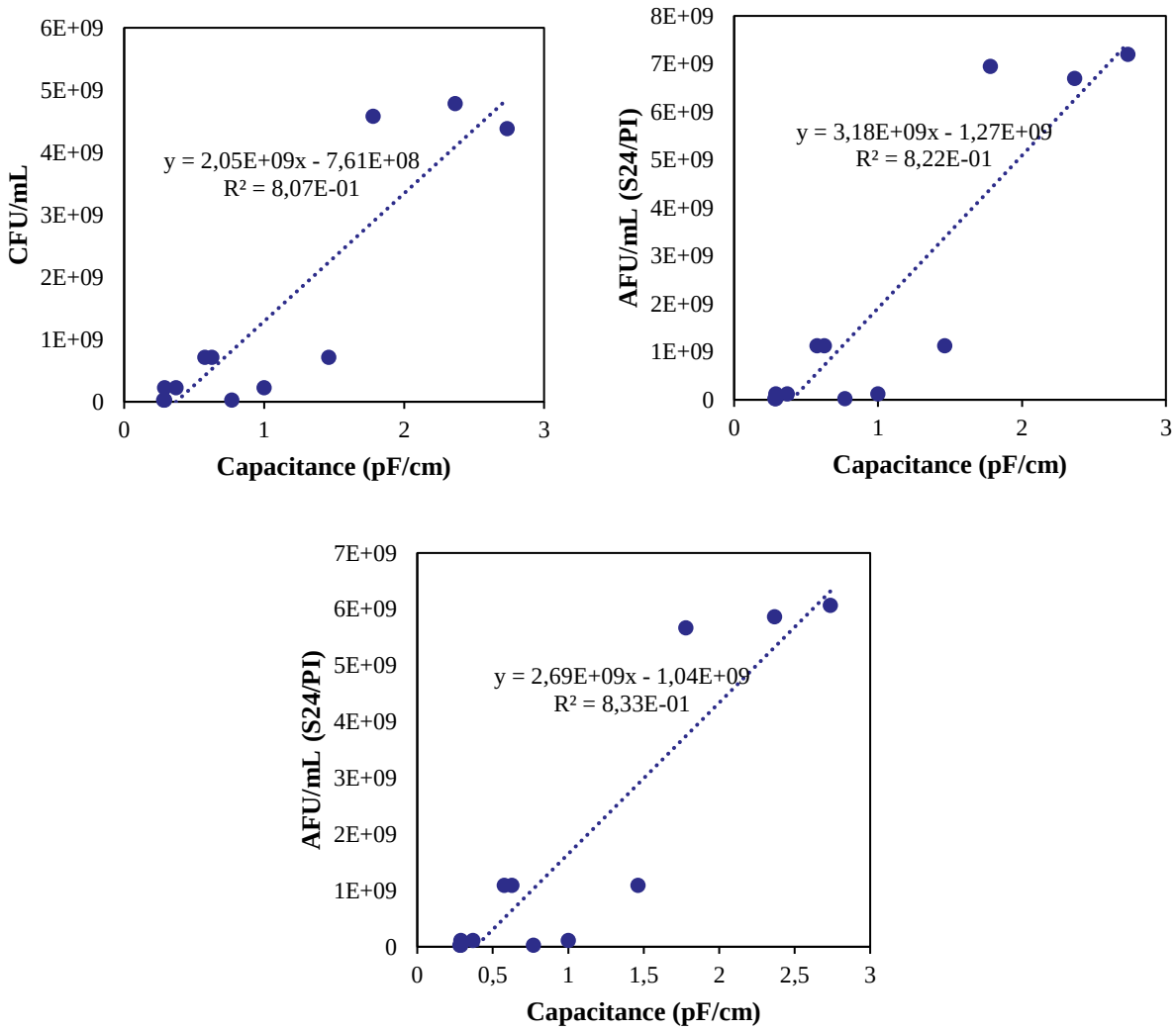

Figure 5.9 Linear correlation during the exponential phase of capacitance measurements at 300 kHz and offline measurements of viable cell density in Colony Forming Units (CFU/mL), and Active Fluorescent Units (AFU/mL) with the methodology of double stain using Syto 24/PI and cFDA/PI. Applied to 1-liter batch fermentations of *B. lactis*.

5.1.3. Model creation for the estimation of the Viable Cell Density

Regardless of the inconsistency in the permittivity and the capacitance measures, the modeling was done. Three models were obtained, each one created with the data of each measurement of viable cell density. It was possible to obtain a file containing the model (Annex) which had two uses: first, it could be registered into the permittivity probes and use it to measure the viable cell density online in future batches. Second, it could be used on the software ArcAir data modeling to evaluate the data of future batches after the end of the fermentation. It was also possible to also obtain a validation report with the statistical performance of the model as presented in Figure 5.10.

The models obtained a good correlation (R^2>0.9) when there were produced by the software (training), but the correlation was not good in every case (R^2<0.9) when the model was in the validation process, and the data dispersion had up to 20% of relative error. Furthermore, the model was not able to predict the behavior in the data of other biological replicates different from those used for the model construction showing the lack of repeatability of the permittivity measurements.

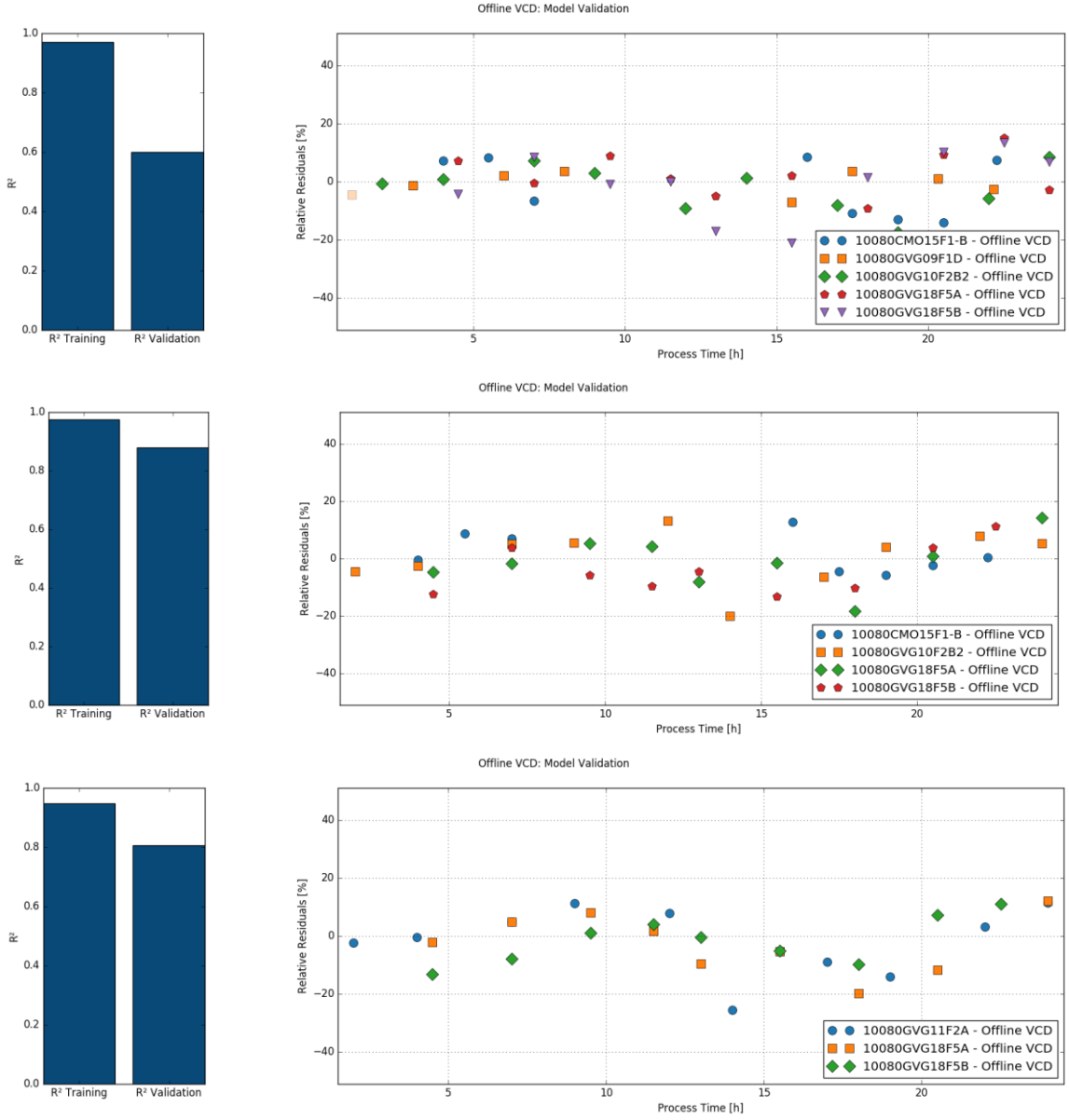

Figure 5.10 Statistical performance of the non-linear models correlating the viable cell density, in CFU/mL (top), in AFU/mL using the Syto24/PI (middle) and cFDA/PI (bottom) methodologies, and the capacitance measurements in 1-liter batch fermentations of *B. lactis*.

5.2. Lactobacillus acidophilus

5.2.1. Kinetic study of the growth and acidification of *L. accidophilus*

The results of the viable cell density determination by viable cell count and flow cytometry with double staining are presented in Figure 5.11.

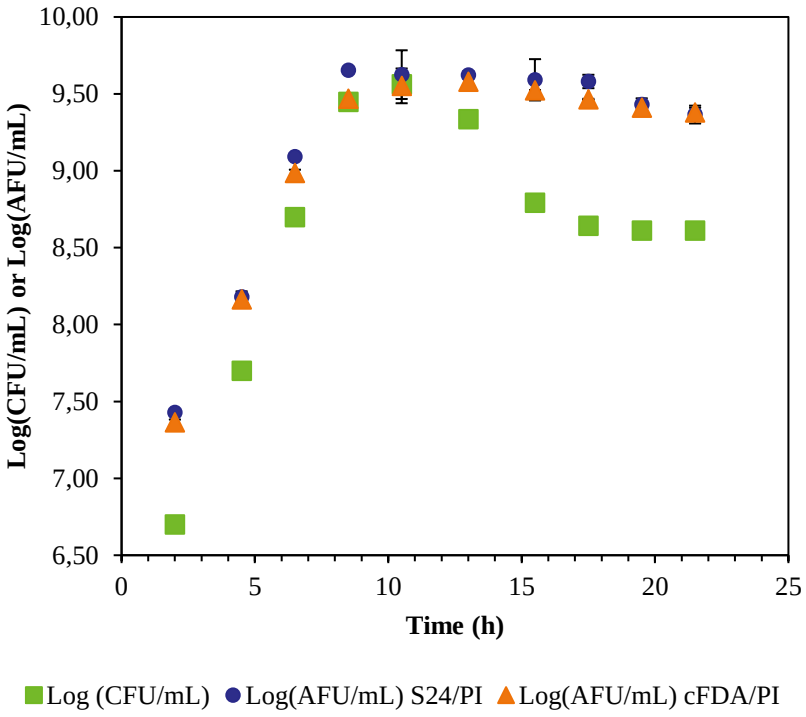

Figure 5.11 Offline measurements for Viable Cell Density of a 1-Liter batch culture of *L. acidophilus*. Viable cell density measured in the logarithm Colony Forming Units (CFU/mL) and Active Fluorescent Units (AFU/mL) with the methodology of double stain using Syto 24/PI and cFDA/PI.

The exponential growth phase of *L. acidophilus* starts 2 hours after the start of the culture, and it prolongates to the 9 hours of culture for the three determinations of viable cell density. The stationary phase prolongates from the 9 hours to the 12 hours, followed by the death phase. During the exponential phase, the cells may regain cultivability since the values of CFU/mL approaches more the AFU/mL values as this phase develops. The AFU/mL and CFU/mL values remain similar during the stationary phase, but they are different during the death phase. The AFU/mL decreased slowly during the death phase meanwhile the CFU/mL suffers a fast reduction which may indicate that the cultivability of the cells is lost, but the viability is maintained.

The optical density presented in Figure 5.12 follows a similar kinetic behavior to the cell viability during the exponential phase, which starts at 2 hours of culture and ends at 10 hours. Afterwards, the stationary

phase prolongates till the end of the fermentation indicating that the biomass total concentration changes minimally.

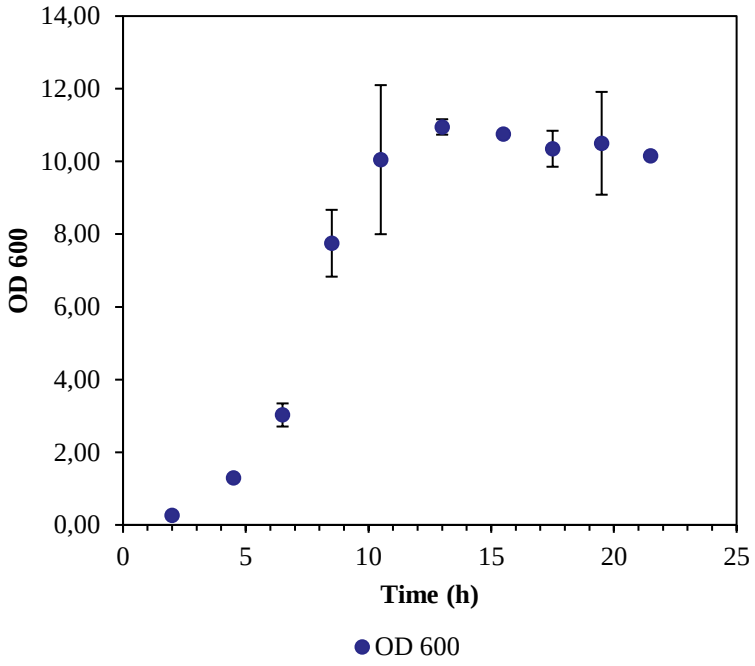

Figure 5.12 Optical density at 600 nm of *L. acidophilus* growth in 1-liter batch culture.

The sugar consumption, the acetate and lactate production during the fermentation are presented in Figure 5.13. The glucose is consumed during 2 and 13 hours of fermentation, and during this period lactic acid is produced exponentially to a maximum at the 13 hours of 36.9 g/L. This maximum of lactate and minimum of glucose concurs with the maximum of optical density, and the beginning of the reduction of cell cultivability which may be explained by the glucose depletion necessary as energy source to maintain the cells. Differently to *B. lactis*, *L acidophilus* do not produce acetic acid, only lactic acid being an homofermentative lactic acid bacteria (Bull et al., 2013).

Due to the sterilization process, 25.6% of the sugar added is transformed to other sugar derivates at the beginning of the fermentation which is detected as fructose or trehalose in the HPLC. However, differently to *B. lactis*, *L. acidophilus* can metabolite these derivatives at the same time as the glucose and it depleted them before the glucose.

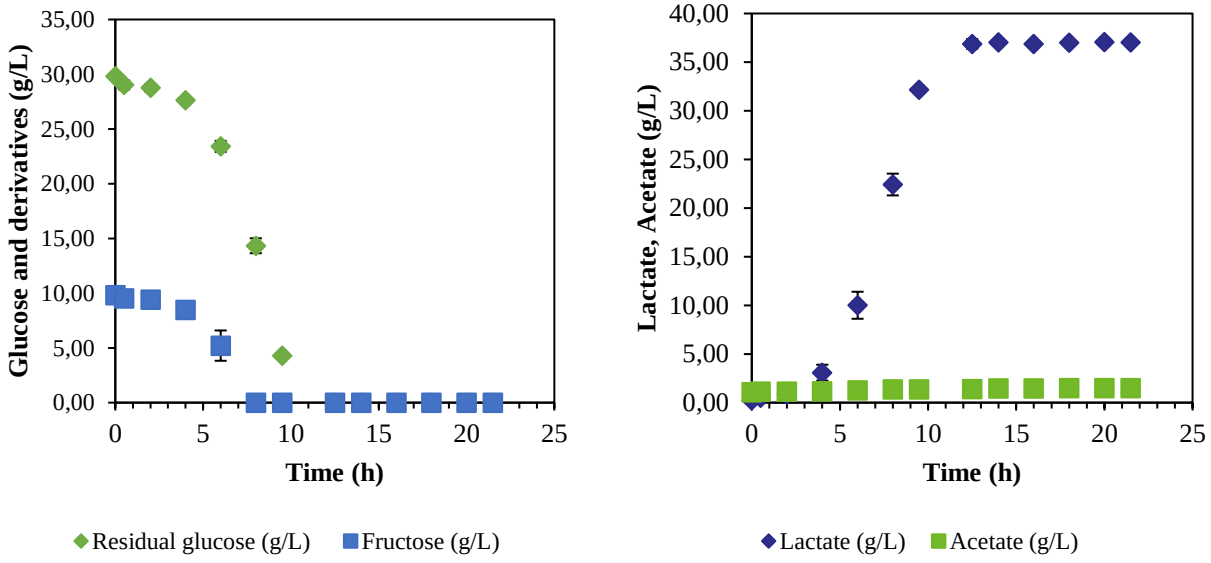

Figure 5.13 Kinetics of glucose consumption (left), acetate and lactate production (right) of a 1-Liter batch culture of *L. acidophilus*.

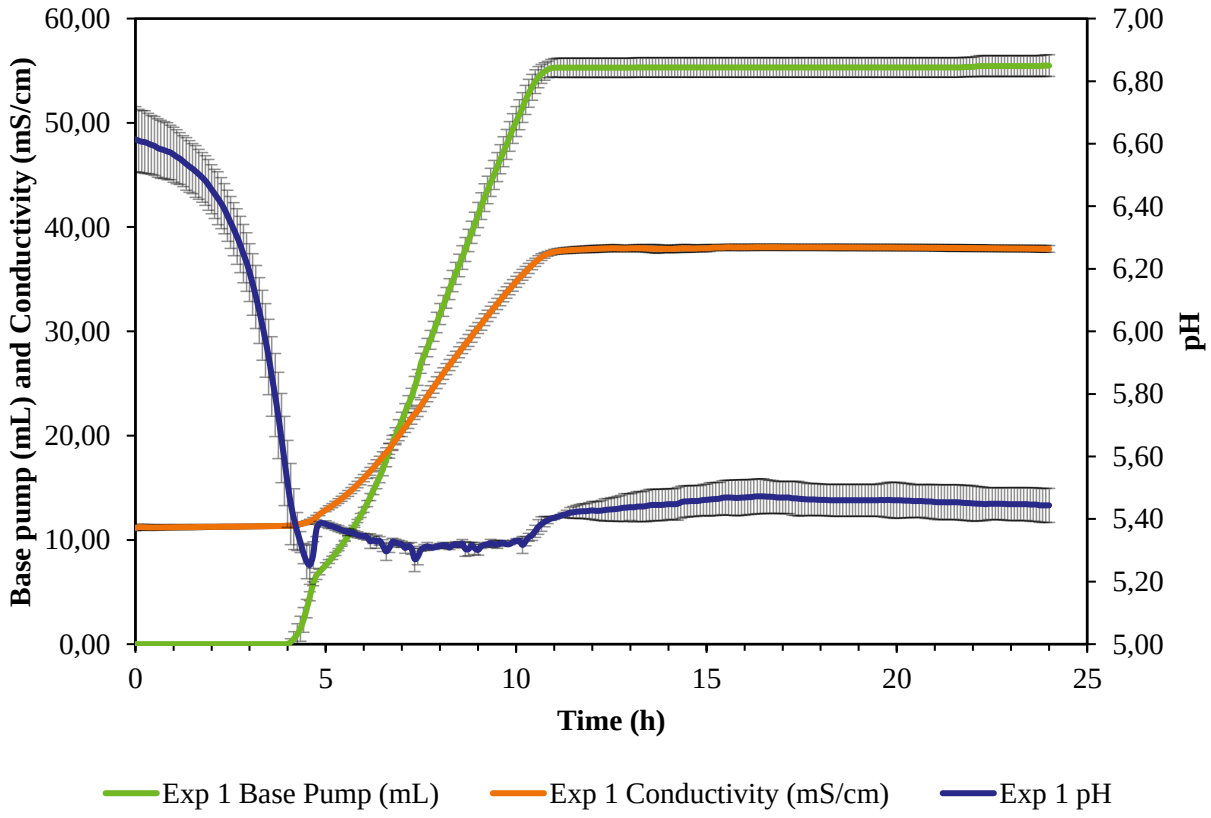

Figure 5.14 Curves of pH, injected base, and conductivity of a 1-liter batch fermentation of *L. acidophilus*.

The curves of pH, base injected and conductivity are presented in Figure 5.14. The culture media undergo a fast reduction of pH between the hours 2 and 4. Afterwards, base is added to stabilize it at 5.5. The

base is added till the 10 hours of culture, time when the cell viability reaches its maximum, the glucose is possibly depleted, and the lactic acid production may stop. The conductivity follows a kinetic behavior comparable to the base addition since this is the one that drives the conductivity augmentation.

5.2.2. Permittivity measurements

Like the experiments with *B. lactis*, the permittivity at 580 kHz and the capacitance at different frequencies from 300 kHz to 10 MHz were obtained from the permittivity probes in each biological replicate. The permittivity curves of 4 biological replicates are presented in Figure 5.15. This time the permittivity measurements were more consistent in three out of four replicates, however, it was not possible to establish a linear correlation with the viable cell density during the exponential phase from 2 to 9 hours of culture.

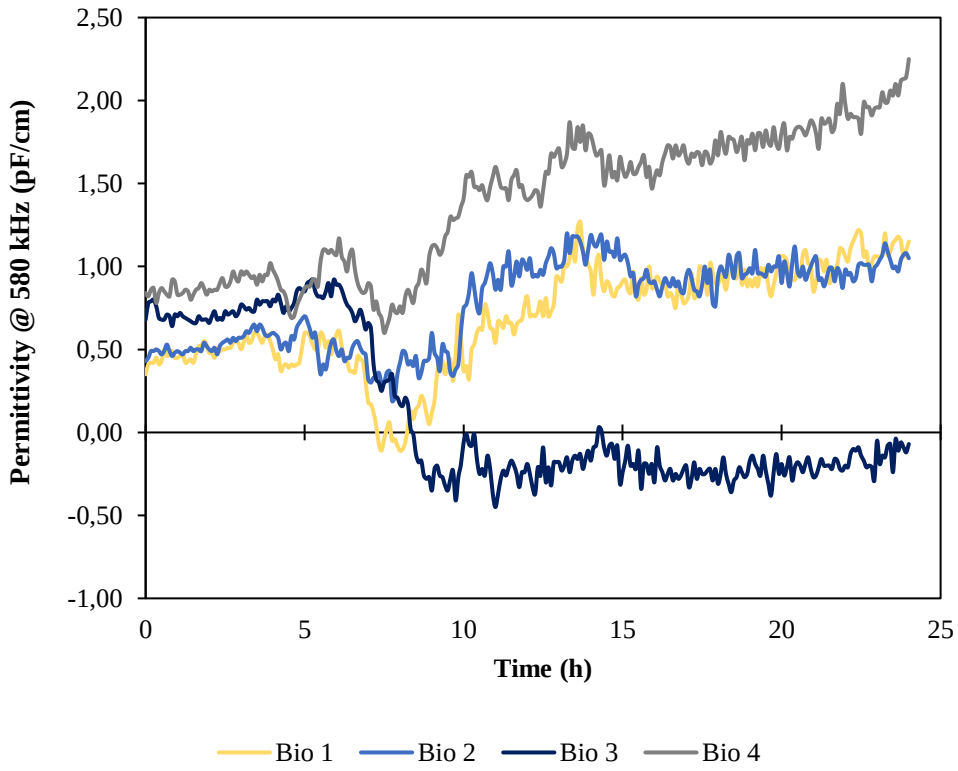

Figure 5.15 Permittivity curves measured at 580 kHz of 4 replicates of 1-liter batch fermentation of *L. acidophilus*.

The culture media capacitance at 300 kHz is presented in Figure 5.16, where it is possible to observe that the kinetic behavior is similar for the same three biological replicates, especially during the exponential phase culture. Besides, the sensitivity of the method was higher since it reached values up to 15 pF/cm while for the measurements of *B. lactis*, the maximum value was around 8.

The linear correlation of the viable cell density of each batch as a function of the capacitance at 300 kHz permittivity was evaluated in Figure 5.17, and in the same three biological replicates the correlation was stablished (R^2>0.95) with each measurement of viable cell density (CFU/mL and AFU/mL with both methodologies).

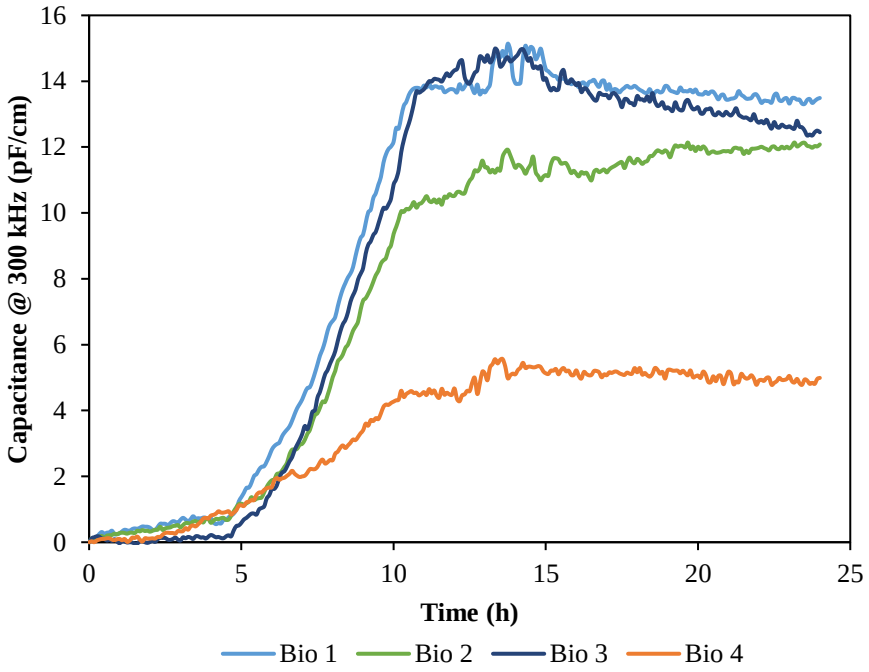

Figure 5.16 Culture media capacitance curves measured at 300 kHz of 4 replicates of 1-liter batch fermentation of *L acidophilus*.

Afterwards, the same linear correlation was evaluated for the points of those three replicates all together (Figure 5.18) and, differently to the experiments with *B. lactis*, a good linear correlation (R^2>0.95) was obtained. Considering the positive results, the modeling was then realized.

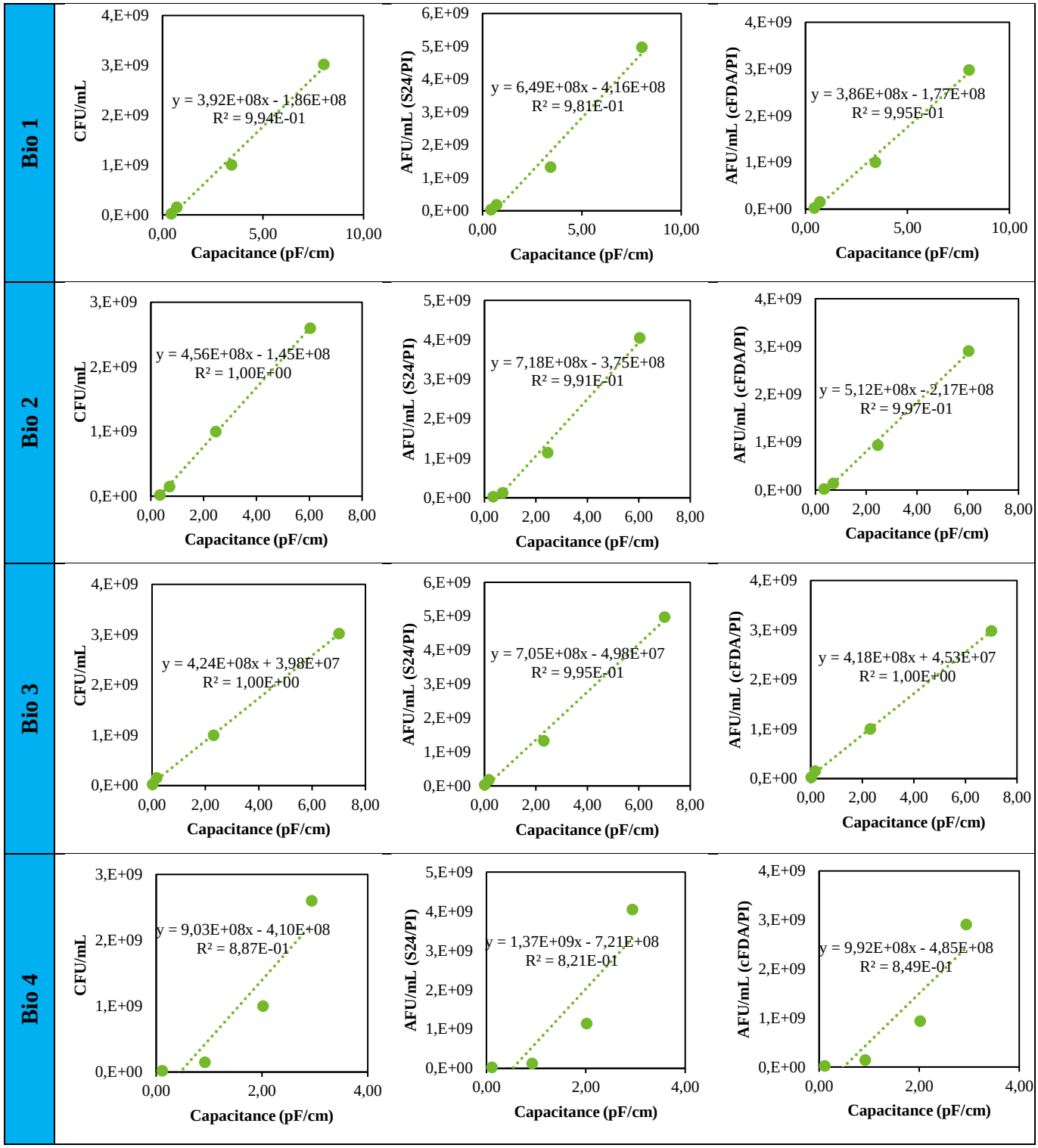

Figure 5.17 Linear correlation of capacitance measurements at 300 kHz and offline measurements of viable cell density in Colony Forming Units (CFU/mL), and Active Fluorescent Units (AFU/mL) with the methodology of double stain using Syto 24/PI and cFDA/PI. Applied to 4 biological replicates of 1-liter batch fermentation of *L. acidophilus*.

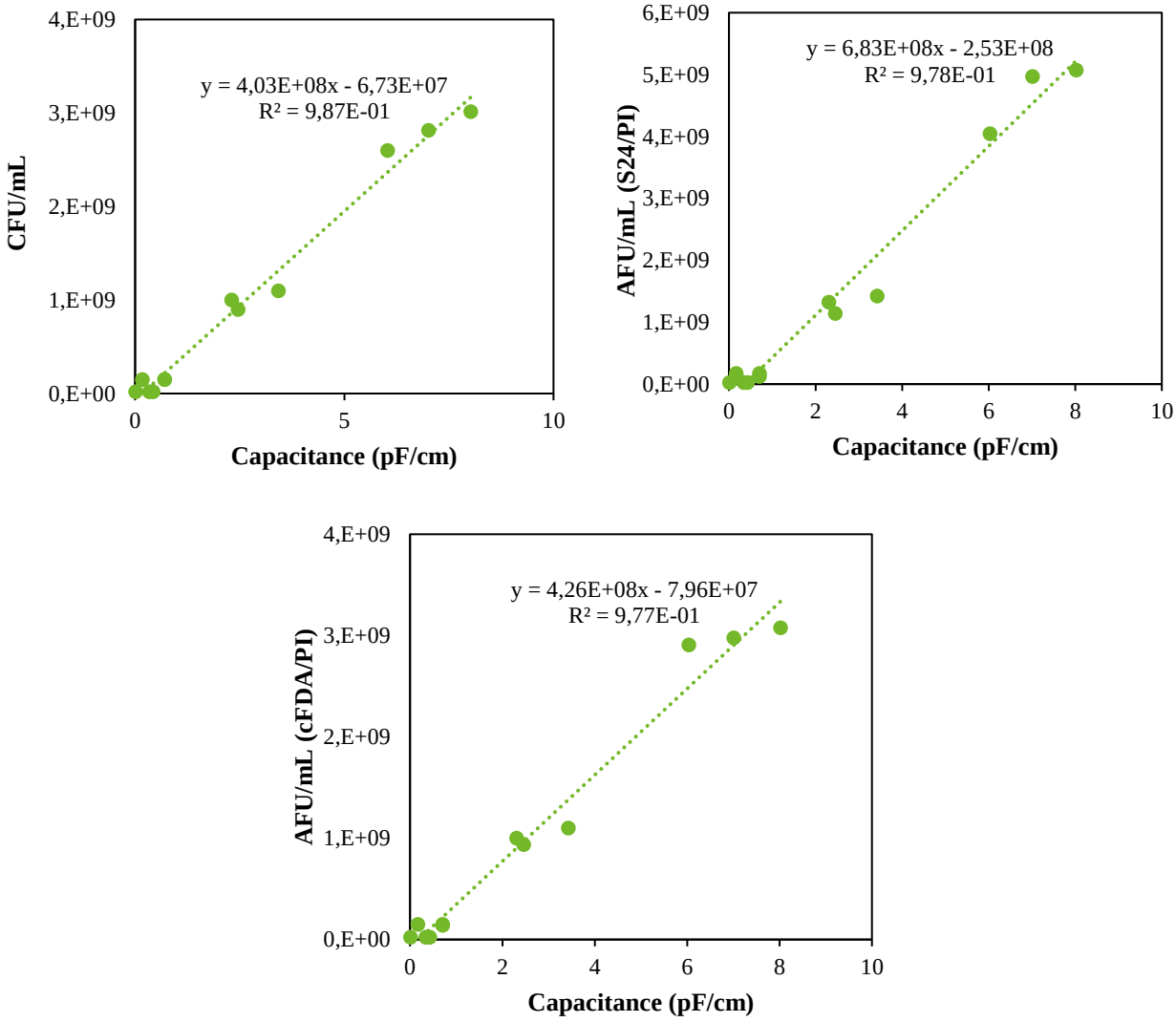

Figure 5.18 Linear correlation of capacitance measurements at 300 kHz and offline measurements of viable cell density in Colony Forming Units (CFU/mL), and Active Fluorescent Units (AFU/mL) with the methodology of double stain using Syto 24/PI and cFDA/PI. Applied to 1-liter batch fermentations of *L. acidophilus*.

5.2.3. Model creation for the estimation of the Viable Cell Density

Three models were obtained as described in the section 5.1.3 with the same characteristics, one for each viable cell density measurement. The file content is presented in the Annex and the validation reports were also produced, and the statistical performance of the models are presented in Figure 5.19.

Despite the repeatability of the results and the good linear correlation during the exponential phase, the models did not have a good correlation (R^2<0.9) when they were produced (training), when they were validated, or in both cases. During the validation, the models had errors up to 50% when comparing the

offline measurements and the online measurements as presented in Figure 5.19. When applied to other data sets, the correlation was also low, and the relative error also reached 50%.

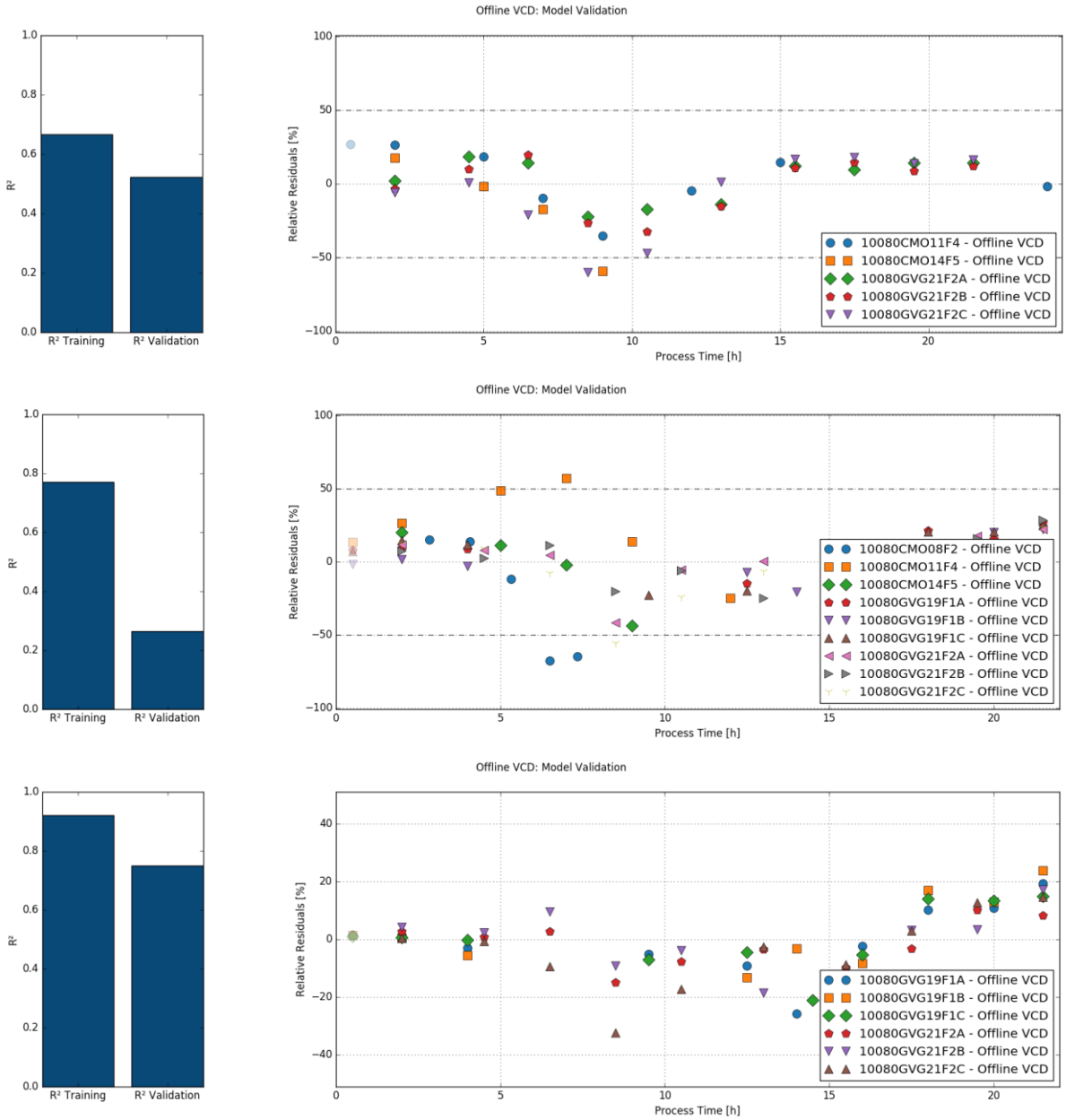

Figure 5.19 Statistical performance of the non-linear models correlating the viable cell density, in CFU/mL (top), in AFU/mL using the Syto24/PI (middle) and cFDA/PI (bottom) methodologies, and the capacitance measurements in 1-liter batch fermentations of *L. acidophilus.*

6. Discussion

Permittivity measurement to estimate the viable cell density has been applied in a myriad of process with mammalian cell culture at laboratory, pilot and industrial scales (Bergin et al., 2022; Justice et al., 2011; Metze et al., 2020). However, its application in microbial bioprocess is limited since the morphology changes that a microorganism suffers through a fermentation modifies the correlation between permittivity and viable cell density (Flores-Cosío et al., 2020). Nevertheless, it has been applied to detect the formation of lipid droplets in yeast, the sporulation of bacteria, and even the viable cell density and cell diameter in *E. coli* (Flores-Cosío et al., 2020; Swaminathan et al., 2022).

In this project, the correlation of viable cell density and permittivity was not successful. The lack of consistency in the permittivity results from one sensor to another and from one run to another did not allow to find a good linear correlation in the experiments with *B. lactis* and it did not allow to build reliable models using both microbial strains (*B. lactis* and *L. acidophilus*). Considering that the rest of the measurements online and offline (viable cell density with three methodologies, optical density, glucose consumption, organic acids production, pH, conductivity, and base added) were repeatable and consistent, the trouble may come from the probes.

A plausible reason of this inconsistency is the electrode polarization effect. This is defined as the accumulation of a spatial charge on the surface of electrodes, causing the formation of an electrical double layer that strongly modifies the ion distribution of the medium. It is caused by a high conductivity, the physicochemical state of the electrode surface, and the ionic species of the medium (Bordi et al., 2001). It masks the properties of the solution including the capacitance and the dielectric dispersion of the cell suspensions, equivalent to the cell size dispersion (Flores-Cosío et al., 2020; Swaminathan et al., 2022). This could explain the high variability in the permittivity measurements, specially when the conductivity increases.

In addition, both strains can adhere to surfaces (Bull et al., 2013; Uusitupa et al., 2020), but specially *B. lactis* was able to create biofilms in the bioreactor during the fermentation. Possibly, a thin biofilm formation around the electrode may have affected the measurements and explain the bad linear correlation between the viable cell density and the culture media capacitance during the exponential phase that theoretically presents a homogeneous morphology.

Another important factor to consider is the optimization of the permittivity probes and the modeling software of the supplier to work specifically with mammalian cells. This may originate that the modeling software is not responsive enough to interpret a substantial change in the morphology that microorganisms suffer during the different growth phases compared to the mammalian cells. Also, it may not do a good interpretation of the substantial change in the cell concentration in a brief time during

the exponential growth phase. This is characteristic of the microbial fermentation, in this case the batch fermentations lasted only one day, meanwhile a mammalian cell culture can take several days (Metze et al., 2020).

To overcome the software limitations, it may be possible to implement another modeling software that do not rely only on coefficients that multiply the capacitance measurements, but also on the Cole-Cole equation, which describes the permittivity behavior at the different frequencies of the β-dispersion. This was previously done for *E. coli* (Swaminathan et al., 2022), and it could provide information not only of the viable cell density, but also about the cell diameter as it was presented in the introduction (1.3.4).

$$\varepsilon(\omega) = \left(\frac{\Delta\varepsilon\left(1 + \left(\frac{\omega}{\omega_c}\right)^{(1-\alpha)} \sin\left(\frac{\pi}{2}\alpha\right)\right)}{1 + \left(\frac{\omega}{\omega_c}\right)^{(2-2\alpha)} + 2\left(\frac{\omega}{\omega_c}\right)^{(1-\alpha)} \sin\left(\frac{\pi}{2}\alpha\right)} + \varepsilon_\infty \right)$$

Eq. 3 Cole-Cole equation that describes β-dispersion of permittivity in biological substances. ε is the permittivity at the frequency ω, ε_∞ is the permittivity at a high frequency after the β-dispersion, Δε is the difference in the permittivity $\varepsilon(\omega) - \varepsilon_\infty$, ω_c is the characteristic frequency where Δε reach half of its maximum value, and α is the angle of the permittivity curve slope at ω_c (Swaminathan et al., 2022).

7. Conclusions and perspectives

The implementation of permittivity measurements to estimate the viable cell density in microbial fermentations have several limitations. First, it is highly dependent of the microbial strain and the physiological state of it. This creates the necessity of creating a non-linear model capable of estimate the viable cell density in different growth phases for each strain, which has the need of running the same experiment several times at 1-Liter bioreactor scale to obtain enough data to build each model. Secondly, the permittivity measurements are subjected to interferences like the electrode polarization, and the deposition of cells in the electrodes, effects that may impact the measurement accuracy.

In this project, 1-Liter 24-hours batch fermentations of lactic acid bacteria of industrial interest, *Bifidobacterium animalis subsp. lactis* and *Lactobacillus acidophilous*, were performed with at least 4 biological replicates. It was possible to obtain the kinetics of acidification, optical density, carbon source consumption, and viable cell density by viable cell count and flux cytometry. The results of these measurements were accurate.

However, the capacitance and permittivity measurements were not accurate from one biological replicate to another. This led to non-linear models that were not able to predict reliably the viable cell density using the capacitance measurements. Nevertheless, it was possible to find a linear correlation between the capacitance at low frequency and the viable cell density during the exponential phase.

To improve these results, it may be possible to use probes more adapted for its use with bacterial cell culture and use a software more adapted to the kinetic behavior of bacterial fermentations including fast changes in the cell concentration and the cell morphology.

Besides, it has been proved that permittivity measurements can be used to detect morphology changes (Flores-Cosío et al., 2020). Hence, the next phase of the project will aim to detect the bacterial sporulation by permittivity and capacitance measurements.

8. Annex

8.1. Files containing the models and the coefficients

8.1.1. *Bifidobacterium animalis subs lactis* with CFU.

{"id": 233, "name": "SB223 CFU A", "extended_name": "SB223 CFU A \u00b7 VCD [e6 cells/ml]", "description": "",
"created_by": "admin", "creation_date": "2023-05-10", "creation_time": "15:01:18",
"modification_time": "2023-05-10T15:01:18.382184Z",
"organism": "bacteria", "organism_name": "Bacteria",
"used_batches": [95, 96, 98, 100, 92], "used_batch_names": ["10080CMO15F1-B",
"10080GVG09F1D", "10080GVG10F2B2", "10080GVG18F5A", "10080GVG18F5B"],
"used_variables": ["C(1118kHz)", "C(1392kHz)", "C(1729kHz)", "C(2155kHz)", "C(2689kHz)",
"C(300kHz)", "C(3347kHz)", "C(374kHz)", "C(4158kHz)", "C(466kHz)", "C(5188kHz)",
"C(580kHz)", "C(6447kHz)", "C(720kHz)", "C(8030kHz)", "C(896kHz)", "C(9995kHz)",
"Conductivity_C(300kHz)"],
"r2_training": 0.970806444096354, "r2_validation": 0.600738260916179,
"responses": ["Offline VCD"], "response_units": ["e6 cells/ml"],
"ridge_intercept": "1386.75127762086",
"ridge_coefficients": ["6930.96442419977", "869.073391811348", "-30364.8879720436",
"9461.22294007491", "14258.622376236", "1713.87295541461", "-29280.1174716428",
"1645.03732643548", "25027.8350472023", "-7852.40664907882", "-5785.72696100347", "-3945.68749615028", "26078.1009048488", "8115.16942912328", "19754.3859536285",
"2808.76986765818", "-40444.8715593897", "0.0"],
"sensor": "incyte", "sensor_name": "Incyte", "enable_interpolation": true,
"enable_use_of_conductivity": false,
"checksum": "0000ec478a11c07f18b125646ceee9d89f9ada390c0c47cf3deccafa3a281603",
"checksum_short": "0000ec478a11c07f18b125646ceee9d8"}

8.1.2. *Bifidobacterium animalis subs lactis* with AFU S24/PI.

{"id": 461, "name": "SB223 AFU S24 A", "extended_name": "SB223 AFU S24 A \u00b7 VCD [e6 cells/ml]", "description": "",
"created_by": "admin", "creation_date": "2023-05-12", "creation_time": "07:50:20",
"modification_time": "2023-05-12T07:50:20.624969Z",
"organism": "bacteria", "organism_name": "Bacteria",

"used_batches": [107, 102, 103, 104], "used_batch_names": ["10080CMO15F1-B", "10080GVG10F2B2", "10080GVG18F5A", "10080GVG18F5B"],
"used_variables": ["C(1118kHz)", "C(1392kHz)", "C(1729kHz)", "C(2155kHz)", "C(2689kHz)", "C(300kHz)", "C(3347kHz)", "C(374kHz)", "C(4158kHz)", "C(466kHz)", "C(5188kHz)", "C(580kHz)", "C(6447kHz)", "C(720kHz)", "C(8030kHz)", "C(896kHz)", "C(9995kHz)", "Conductivity_C(300kHz)"],
"r2_training": 0.974626449119671, "r2_validation": 0.879908713820856,
"responses": ["Offline VCD"], "response_units": ["e6 cells/ml"],
"ridge_intercept": "-24946.2299014815",
"ridge_coefficients": ["-17144.2446180751", "5704.73637971881", "-294.864736337314", "31296.3190343945", "-1021.9904800851", "1656.81911751175", "-15596.6995112893", "9407.60628229514", "-2167.3162444814", "-19180.8507796748", "687.966072745872", "-2447.7664959717", "17986.0287139604", "-6824.87890691865", "-14589.08317275", "23971.4436677829", "-12196.8787652357", "1240.35418906909"],
"sensor": "incyte", "sensor_name": "Incyte",
"enable_interpolation": false, "enable_use_of_conductivity": true,
"checksum": "1a010091385c9acc567cb98e1b116c8a6565ab8d2597a32aaf774e5c089c977d",
"checksum_short": "1a010091385c9acc567cb98e1b116c8a"}

8.1.3. *Bifidobacterium animalis subs lactis* with AFU cFDA/PI.

{"id": 531, "name": "SB223 AFU cFDA A", "extended_name": "SB223 AFU cFDA A \u00b7 VCD [e6 cells/ml]", "description": "",
"created_by": "admin", "creation_date": "2023-05-12", "creation_time": "08:22:30",
"modification_time": "2023-05-12T08:22:30.303969Z",
"organism": "bacteria", "organism_name": "Bacteria",
"used_batches": [101, 103, 104], "used_batch_names": ["10080GVG11F2A", "10080GVG18F5A", "10080GVG18F5B"],
"used_variables": ["C(1118kHz)", "C(1392kHz)", "C(1729kHz)", "C(2155kHz)", "C(2689kHz)", "C(300kHz)", "C(3347kHz)", "C(374kHz)", "C(4158kHz)", "C(466kHz)", "C(5188kHz)", "C(580kHz)", "C(6447kHz)", "C(720kHz)", "C(8030kHz)", "C(896kHz)", "C(9995kHz)", "Conductivity_C(300kHz)"],
"r2_training": 0.94802313125129, "r2_validation": 0.805839719089271,
"responses": ["Offline VCD"], "response_units": ["e6 cells/ml"],
"ridge_intercept": "-7712.88366413004",
"ridge_coefficients": ["-6316.10148363546", "746.687864143881", "-634.02124330198", "1864.09489220353", "-789.915632985018", "451.84486976957", "-8214.3257685814", "543.128199331922", "-5544.51244101589", "126.655729330811", "6103.35401517788", "-

1024.05007246929", "3149.68368320907", "1324.34910691991", "8649.80541973052",
"1395.42025386871", "2965.63454465017", "0.0"],
"sensor": "incyte", "sensor_name": "Incyte",
"enable_interpolation": false, "enable_use_of_conductivity": false,
"checksum": "134d720a5971e484802241c30846fa0ec412336a72e2708550c897a4d1213885",
"checksum_short": "134d720a5971e484802241c30846fa0e"}

8.1.4. *Lactobacillus acidophilus* with CFU.

{"id": 1013, "name": "SB47 CFU A", "extended_name": "SB47 CFU A \u00b7 VCD [e6 cells/ml]",
"description": "",
"created_by": "admin", "creation_date": "2023-05-31", "creation_time": "10:16:57",
"modification_time": "2023-05-31T10:16:57.891924Z",
"organism": "bacteria", "organism_name": "Bacteria",
"used_batches": [116, 109, 120, 117, 118], "used_batch_names": ["10080CMO11F4",
"10080CMO14F5", "10080GVG21F2A", "10080GVG21F2B", "10080GVG21F2C"],
"used_variables": ["C(1118kHz)", "C(1392kHz)", "C(1729kHz)", "C(2155kHz)", "C(2689kHz)",
"C(300kHz)", "C(3347kHz)", "C(374kHz)", "C(4158kHz)", "C(466kHz)", "C(5188kHz)",
"C(580kHz)", "C(6447kHz)", "C(720kHz)", "C(8030kHz)", "C(896kHz)", "C(9995kHz)",
"Conductivity_C(300kHz)"],
"r2_training": 0.666552304200553, "r2_validation": 0.523300614108495,
"responses": ["Offline VCD"], "response_units": ["e6 cells/ml"],
"ridge_intercept": "1024.51818115741",
"ridge_coefficients": ["44.4807319965674", "-1910.74409922116", "452.454388846006",
"1763.10571193002", "2972.09061186183", "329.827436192038", "2959.68829215747",
"646.75842826605", "1271.87680481206", "631.172382153313", "388.444360063791", "-
781.576489199504", "72.8973427897532", "-1608.55078792275", "-1246.36487342071", "-
3322.85235068154", "-3383.30852660466", "0.0"],
"sensor": "incyte", "sensor_name": "Incyte",
"enable_interpolation": true, "enable_use_of_conductivity": false,
"checksum": "35ba2417880e9e011151e59cb6c2d8e6ddd3c580fa56fd16a6fc4814869161f8",
"checksum_short": "35ba2417880e9e011151e59cb6c2d8e6"}

8.1.5. *Lactobacillus acidophilus* with AFU S24/PI.

{"id": 967, "name": "SB47 AFU S24 A", "extended_name": "SB47 AFU S24 A \u00b7 VCD [e6 cells/ml]", "description": "",
"created_by": "admin", "creation_date": "2023-05-31", "creation_time": "10:01:33",
"modification_time": "2023-05-31T10:01:33.662924Z",
"organism": "bacteria", "organism_name": "Bacteria",
"used_batches": [114, 116, 109, 110, 111, 112, 120, 117, 118], "used_batch_names": ["10080CMO08F2", "10080CMO11F4", "10080CMO14F5", "10080GVG19F1A", "10080GVG19F1B", "10080GVG19F1C", "10080GVG21F2A", "10080GVG21F2B", "10080GVG21F2C"],
"used_variables": ["C(1118kHz)", "C(1392kHz)", "C(1729kHz)", "C(2155kHz)", "C(2689kHz)", "C(300kHz)", "C(3347kHz)", "C(374kHz)", "C(4158kHz)", "C(466kHz)", "C(5188kHz)", "C(580kHz)", "C(6447kHz)", "C(720kHz)", "C(8030kHz)", "C(896kHz)", "C(9995kHz)", "Conductivity_C(300kHz)"],
"r2_training": 0.7710653403285, "r2_validation": 0.263700750452739,
"responses": ["Offline VCD"], "response_units": ["e6 cells/ml"],
"ridge_intercept": "383.585250054912",
"ridge_coefficients": ["-366.543294582428", "-427.697653262986", "-1781.27078534123", "-5341.85956816785", "1876.40968931261", "-642.068928410452", "-2296.47150007375", "-1044.75556562678", "3915.3415986954", "3650.0467062242", "10821.8468023091", "1594.91664060032", "3636.45215287476", "-1655.32089371297", "-2609.18864927475", "-1673.32849917598", "-7587.26564596619", "0.0"],
"sensor": "incyte", "sensor_name": "Incyte",
"enable_interpolation": false, "enable_use_of_conductivity": false,
"checksum": "a0acc1cbb164ba14138fb7756d31e6f02d8d1007f77e909a3df018bbe8184f8b",
"checksum_short": "a0acc1cbb164ba14138fb7756d31e6f0"}

8.1.6. *Lactobacillus acidophilus* with AFU cFDA/PI.

{"id": 1225, "name": "SB47 SFU cFDA A", "extended_name": "SB47 SFU cFDA A \u00b7 VCD [e6 cells/ml]", "description": "",
"created_by": "admin", "creation_date": "2023-06-01", "creation_time": "08:51:01",
"modification_time": "2023-06-01T08:51:01.039466Z",
"organism": "bacteria", "organism_name": "Bacteria",
"used_batches": [110, 111, 112, 120, 117, 118], "used_batch_names": ["10080GVG19F1A", "10080GVG19F1B", "10080GVG19F1C", "10080GVG21F2A", "10080GVG21F2B", "10080GVG21F2C"],

"used_variables": ["C(1118kHz)", "C(1392kHz)", "C(1729kHz)", "C(2155kHz)", "C(2689kHz)", "C(300kHz)", "C(3347kHz)", "C(374kHz)", "C(4158kHz)", "C(466kHz)", "C(5188kHz)", "C(580kHz)", "C(6447kHz)", "C(720kHz)", "C(8030kHz)", "C(896kHz)", "C(9995kHz)", "Conductivity_C(300kHz)"],
"r2_training": 0.920663154720504, "r2_validation": 0.74953825254109,
"responses": ["Offline VCD"], "response_units": ["e6 cells/ml"],
"ridge_intercept": "-158.661428663929",
"ridge_coefficients": ["-751.752855425842", "3595.36670689872", "-3867.9229022647", "514.229917736526", "-1218.65893754957", "-435.772035776784", "-1860.02787898098", "293.871681249894", "4741.52085525108", "1335.72673313907", "2697.602643061", "726.799773823713", "2694.60645773093", "-2992.05218816301", "-1665.05193096196", "-324.808826968297", "-3758.17067354078", "85.6250608650327"],
"sensor": "incyte", "sensor_name": "Incyte",
"enable_interpolation": false, "enable_use_of_conductivity": true,
"checksum": "b7a7a623d7461049edf10197439628d96a787520c9d9090446980891fd7c1031",
"checksum_short": "b7a7a623d7461049edf10197439628d9"}

9. References

Araujo, L. D. C., Furlaneto, F. A. C., da Silva, L. A. B., & Kapila, Y. L. (2022). Use of the Probiotic Bifidobacterium animalis subsp. Lactis HN019 in Oral Diseases. *International Journal of Molecular Sciences*, *23*(16), 9334. https://doi.org/10.3390/ijms23169334

Baymiev, An. Kh., Baymiev, Al. Kh., Kuluev, B. R., Shvets, K. Yu., Yamidanov, R. S., Matniyazov, R. T., Chemeris, D. A., Zubov, V. V., Alekseev, Ya. I., Mavzyutov, A. R., Ivanenkov, Ya. A., & Chemeris, A. V. (2020). Modern Approaches to Differentiation of Live and Dead Bacteria Using Selective Amplification of Nucleic Acids. *Microbiology*, *89*(1), 13-27. https://doi.org/10.1134/S0026261720010038

Bergin, A., Carvell, J., & Butler, M. (2022). Applications of bio-capacitance to cell culture manufacturing. *Biotechnology Advances*, *61*, 108048. https://doi.org/10.1016/j.biotechadv.2022.108048

Bordi, F., Cametti, C., & Gili, T. (2001) Reduction of the contribution of electrode polarization effects in the radiowave dielectric measurements of highly conductive biological cell suspensions. *Bioelectrochemistry*, *54*, 53-61. https://doi.org/10.1016/S1567-5394(01)00110-4

Bull, M., Plummer, S., Marchesi, J., & Mahenthiralingam, E. (2013). The life history of *Lactobacillus acidophilus* as a probiotic: A tale of revisionary taxonomy, misidentification and commercial success. *FEMS Microbiology Letters*, *349*(2), 77-87. https://doi.org/10.1111/1574-6968.12293

Cheng, J., Laitila, A., & Ouwehand, A. C. (2021). Bifidobacterium animalis subsp. lactis HN019 Effects on Gut Health: A Review. *Frontiers in Nutrition*, *8*, 790561. https://doi.org/10.3389/fnut.2021.790561

Chiron, C., Tompkins, T. A., & Burguière, P. (2018). Flow cytometry: A versatile technology for specific quantification and viability assessment of micro-organisms in multistrain probiotic products. *Journal of Applied Microbiology*, *124*(2), 572-584. https://doi.org/10.1111/jam.13666

Czaplewski, L., Bax, R., Clokie, M., Dawson, M., Fairhead, H., Fischetti, V. A., Foster, S., Gilmore, B. F., Hancock, R. E. W., Harper, D., Henderson, I. R., Hilpert, K., Jones, B. V., Kadioglu, A., Knowles, D., Ólafsdóttir, S., Payne, D., Projan, S., Shaunak, S., … Rex, J. H. (2016). Alternatives to antibiotics—A pipeline portfolio review. *The Lancet Infectious Diseases*, *16*(2), 239-251. https://doi.org/10.1016/S1473-3099(15)00466-1

Díaz, M., Herrero, M., García, L. A., & Quirós, C. (2010). Application of flow cytometry to industrial microbial bioprocesses. *Biochemical Engineering Journal*, *48*(3), 385-407. https://doi.org/10.1016/j.bej.2009.07.013

Flores-Cosío, G., Herrera-López, E. J., Arellano-Plaza, M., Gschaedler-Mathis, A., Kirchmayr, M., & Amaya-Delgado, L. (2020). Application of dielectric spectroscopy to unravel the physiological state of microorganisms: Current state, prospects and limits. *Applied Microbiology and Biotechnology*, *104*(14), 6101-6113. https://doi.org/10.1007/s00253-020-10677-x

Gao, H., Li, X., Chen, X., Hai, D., Wei, C., Zhang, L., & Li, P. (2022). The Functional Roles of *Lactobacillus acidophilus* in Different Physiological and Pathological Processes. *Journal of Microbiology and Biotechnology*, *32*(10), 1226-1233. https://doi.org/10.4014/jmb.2205.05041

Hill, C., Guarner, F., Reid, G., Gibson, G. R., Merenstein, D. J., Pot, B., Morelli, L., Canani, R. B., Flint, H. J., Salminen, S., Calder, P. C., & Sanders, M. E. (2014). The International Scientific Association for Probiotics and Prebiotics consensus statement on the scope and appropriate use of the term probiotic. *Nature Reviews Gastroenterology & Hepatology*, *11*(8), 506-514. https://doi.org/10.1038/nrgastro.2014.66

Iwamoto, M. (2012). Maxwell–Wagner Effect. En B. Bhushan (Ed.), *Encyclopedia of Nanotechnology* (pp. 1276-1285). Springer Netherlands. https://doi.org/10.1007/978-90-481-9751-4_5

Jungersen, M., Wind, A., Johansen, E., Christensen, J., Stuer-Lauridsen, B., & Eskesen, D. (2014). The Science behind the Probiotic Strain Bifidobacterium animalis subsp. Lactis BB-12®. *Microorganisms*, *2*(2), 92-110. https://doi.org/10.3390/microorganisms2020092

Justice, C., Brix, A., Freimark, D., Kraume, M., Pfromm, P., Eichenmueller, B., & Czermak, P. (2011). Process control in cell culture technology using dielectric spectroscopy. *Biotechnology Advances*, *29*(4), 391-401. https://doi.org/10.1016/j.biotechadv.2011.03.002

Knabben, I. (2011). Linear Correlation between Online Capacitance and Offline Biomass Measurement up to High Cell Densities in Escherichia coli Fermentations in a Pilot-Scale Pressurized Bioreactor. *Journal of Microbiology and Biotechnology*, *21*(2), 204-211. https://doi.org/10.4014/jmb.1004.04032

Kumar, S. S., & Ghosh, A. R. (2019). Assessment of bacterial viability: A comprehensive review on recent advances and challenges. *Microbiology*, *165*(6), 593-610. https://doi.org/10.1099/mic.0.000786

Lesaffre (2023). Retrieved on 11/06/2023 from www.lesaffre.com.

Markx, G. H., & Davey, C. L. (1999). The dielectric properties of biological cells at radiofrequencies: Applications in biotechnology. *Enzyme and Microbial Technology*, *25*(3-5), 161-171. https://doi.org/10.1016/S0141-0229(99)00008-3

Metze, S., Blioch, S., Matuszczyk, J., Greller, G., Grimm, C., Scholz, J., & Hoehse, M. (2020). Multivariate data analysis of capacitance frequency scanning for online monitoring of viable cell concentrations in small-scale bioreactors. *Analytical and Bioanalytical Chemistry*, *412*(9), 2089-2102. https://doi.org/10.1007/s00216-019-02096-3

Oliver, J. D. (2005). The Viable but Nonculturable State in Bacteria. *J. Microbiol.*, *43*(S).

O'Neill, J. (2014). *Antimicrobial Resistance: Tackling a Crisis for the Health and Wealth of Nations*. Review on Antimicrobial Resistance.

Papadopoulou, C.-I., Loizou, E., & Chatzitheodoridis, F. (2022). Priorities in Bioeconomy Strategies: A Systematic Literature Review. *Energies*, *15*(19), 7258. https://doi.org/10.3390/en15197258

Procelys (2023). Retrieved on 11/06/2023 from procelys.com

Sanders, M. E., Merenstein, D., Merrifield, C. A., & Hutkins, R. (2018). Probiotics for human use. *Nutrition Bulletin*, *43*(3), 212-225. https://doi.org/10.1111/nbu.12334

Shah, N. P. (2000). Probiotic Bacteria: Selective Enumeration and Survival in Dairy Foods. *Journal of Dairy Science*, *83*(4), 894-907. https://doi.org/10.3168/jds.S0022-0302(00)74953-8

Siano, S. A. (1997). Biomass measurement by inductive permittivity. *Biotechnology and Bioengineering*, *55*(2), 289-304. https://doi.org/10.1002/(SICI)1097-0290(19970720)55:2<289::AID-BIT7>3.0.CO;2-E

Swaminathan, N., Priyanka, P., Rathore, A. S., Sivaprakasam, S., & Subbiah, S. (2022). Cole-Cole modeling of real-time capacitance data for estimation of cell physiological properties in recombinant *Escherichia coli* cultivation. *Biotechnology and Bioengineering*, *119*(3), 922-935. https://doi.org/10.1002/bit.28028

Tang, W. L., & Zhao, H. (2009). Industrial biotechnology: Tools and applications. *Biotechnology Journal*, *4*(12), 1725-1739. https://doi.org/10.1002/biot.200900127

United Nations. (2022). *World Population Prospects 2022: Summary of Results*. United Nations Department of Economic and Social Affairs, Population Division. UN DESA/POP/2022/TR/NO. 3.

Uusitupa, H.-M., Rasinkangas, P., Lehtinen, M. J., Mäkelä, S. M., Airaksinen, K., Anglenius, H., Ouwehand, A. C., & Maukonen, J. (2020). Bifidobacterium animalis subsp. lactis 420 for Metabolic Health: Review of the Research. *Nutrients*, *12*(4), 892. https://doi.org/10.3390/nu12040892

Wagemann, K., & Tippkötter, N. (Eds.). (2019). *Biorefineries* (Vol. 166). Springer International Publishing. https://doi.org/10.1007/978-3-319-97119-3

Wendel, U. (2022). Assessing Viability and Stress Tolerance of Probiotics—A Review. *Frontiers in Microbiology*, *12*, 818468. https://doi.org/10.3389/fmicb.2021.818468

Wilkinson, M. G. (2018). Flow cytometry as a potential method of measuring bacterial viability in probiotic products: A review. *Trends in Food Science & Technology*, *78*, 1-10. https://doi.org/10.1016/j.tifs.2018.05.006

Yu, L., Wu, F., & Chen, G. (2019). Next-Generation Industrial Biotechnology-Transforming the Current Industrial Biotechnology into Competitive Processes. *Biotechnology Journal*, *14*(9), 1800437. https://doi.org/10.1002/biot.201800437